
A Universal Approximation Theorem for Nonlinear Resistive Networks

Benjamin Scellier¹ Siddhartha Mishra²

Abstract

Resistor networks have recently attracted interest as analog computing platforms for machine learning, particularly due to their compatibility with the Equilibrium Propagation training framework. In this work, we explore the computational capabilities of these networks. We prove that electrical networks consisting of voltage sources, linear resistors, diodes, and voltage-controlled voltage sources (VCVS) can approximate any continuous function to arbitrary precision. Central to our proof is a method for translating a ReLU neural network into an approximately equivalent electrical network comprising these four elements. Our proof relies on two assumptions: (a) circuit elements are ideal, and (b) variable resistor conductances and VCVS amplification factors can take any value (arbitrarily small or large). Our findings provide insights that could guide the development of universal self-learning electrical networks.

1. Introduction

Machine learning (ML) is increasingly prevalent in industrial and commercial applications, with neural networks being central to these ML systems. A fundamental characteristic of neural networks is their ability to implement or approximate arbitrary functions: they are universal function approximators. However, training and deploying neural networks on GPUs is energy-intensive, primarily due to the separation of computation and memory in GPUs. As the need for energy-efficient ML systems becomes pressing, researchers explore alternative physical substrates based on analog physics as a replacement for GPU-based neural networks (Momeni et al., 2024). One key area of research has been the development of analog electrical versions of neural networks, which aim to implement their arithmetic operations – including matrix-vector multiplications (MVMs) and nonlinear activation functions – and the backpropaga-

tion (BP) algorithm in the analog domain. However, these systems are typically mixed-signal (analog/digital), executing the nonlinear activation functions in the digital domain, and therefore necessitating the use of analog-to-digital converters (ADCs) and digital-to-analog converters (DACs) (Xiao et al., 2020). This hurdle has motivated researchers to develop and explore alternative training frameworks, potentially better suited for training analog physical systems (Scellier & Bengio, 2017; Scellier et al., 2022; Stern et al., 2021; Wright et al., 2022; Lopez-Pastor & Marquardt, 2023; Wanjura & Marquardt, 2024a; Momeni et al., 2023) – for recent reviews, see also Momeni et al. (2024) and Stern & Murugan (2023). However, the physical systems compatible with these training frameworks are typically not isomorphic to neural networks. In particular, unlike neural networks, the computational capabilities and expressivity of these systems remain largely unexplored, and the features required to make them universal function approximators are currently unknown.

We investigate the question of universal function approximation within the context of resistor networks. These electrical networks are composed of variable resistors (memristors) that serve as trainable weights and voltage sources representing input variables. The steady state of such electrical networks is characterized by the principle of least power dissipation. Although resistor networks have been studied as platforms for analog computing since the 1980s (Harris et al., 1989), their applications were initially limited to inference tasks. More recently, the equilibrium propagation (EP) framework (Scellier & Bengio, 2017; Kendall et al., 2020) has reignited interest in these networks, providing a method to train them. EP uses local contrastive learning rules to adjust the resistor (or memristor) conductances to perform gradient descent on a cost function (Kendall et al., 2020; Anisetti et al., 2024). Experimental implementations of resistor networks that self-train using local learning rules closely related to EP have also been realized (Dillavou et al., 2022; 2024), demonstrating the feasibility of this approach. Additionally, an experimental demonstration on a memristor crossbar array (Yi et al., 2023) suggests potential energy savings of up to four orders of magnitude compared to neural networks trained on GPUs. Importantly, EP is also applicable in nonlinear networks, without requiring detailed knowledge of the nonlinear elements’ characteristics – see

¹Rain AI, San Francisco, USA ²SAM, D-Math and ETH AI Center, ETH Zurich, Switzerland. Correspondence to: Benjamin Scellier <benjamin@rain.ai>.

Appendix E for details. These and other studies (Wycoff et al., 2022; Stern et al., 2022; 2024a;b; Kiraz et al., 2022; Watfa et al., 2023; Oh et al., 2023) have renewed interest in resistor networks. However, the computational expressivity of these networks has remained unexplored.

In this paper, we derive sufficient conditions for resistor networks to be universal function approximators. Clearly, ohmic resistors and ideal voltage sources alone can only implement linear functions. Nonlinear computation, which is a prerequisite for any sort of universal computation, requires nonlinear elements. Furthermore, in a network with only voltage sources and passive (linear or nonlinear) resistors, the voltage across any branch is bounded by the sum of the voltages from the sources (see Appendix B for details). Following Kendall et al. (2020), we address these two issues using diodes for nonlinearities, and voltage-controlled voltage sources (VCVS) for amplification, allowing the implementation of functions with output voltages greater than input voltages. We prove that, under suitable assumptions, these four elements - ohmic resistors, voltage sources, diodes and VCVS - are sufficient for universal function approximation. The assumptions are that (a) the elements are ideal, and (b) the conductances of variable resistors and the amplification factors of the VCVSs can take arbitrary values (arbitrarily small or arbitrarily large). To prove this result, we consider a specific nonlinear resistive network architecture similar to the one proposed by Kendall et al. (2020) which we refer to as a ‘deep resistive network’ (DRN), and we show that DRNs can approximate ReLU neural networks to arbitrary accuracy. Since ReLU neural networks are known to be universal function approximators (Leshno et al., 1993; Yarotsky, 2017), it follows that DRNs are universal approximators, too. Our work thus presents the first universal approximation result for a class of analog electrical networks compatible with EP. Additionally, our proof offers a systematic method for translating a ReLU neural network into an equivalent-sized approximate DRN. We also show that these four elements (ohmic resistors, voltage sources, diodes and VCVS) are required for universal function approximation, in a sense specified in Appendix B.

We emphasize that, in our construction, DRNs do not *implement* ReLU neural networks but rather *approximate* them, in contrast to traditional research on analog electrical neural networks that use BP for training. Furthermore, although in this work we assume ideal elements to simplify the mathematical analysis of DRNs, EP does not require these assumptions. In fact, EP is agnostic to the characteristics of untrainable components such as diodes (See Appendix E for details).

2. Nonlinear resistive networks

We consider an electrical circuit composed of voltage sources, linear resistors, diodes and voltage-controlled voltage sources (Figure 1). We call such a circuit a ‘nonlinear resistive network’. It implements an input-output function as follows: a) a set of voltage sources serve as ‘input variables’ where voltages play the role of input values, and b) a set of branches serve as ‘output variables’ where voltage drops play the role of the model’s prediction. Computing with this electrical network proceeds as follows:

1. set the input voltage sources to input values,
2. let the electrical network reach steady state (the DC operating point of the circuit),
3. read the output voltages across output branches.

The steady state of the network is the configuration of branch voltages and branch currents that verifies all the branch equations, as well as Kirchhoff’s current law (KCL) at every node, and Kirchhoff’s voltage law (KVL) in every loop. We note that some conditions on the network topology and branch characteristics must be met to ensure that there exists a steady state: for instance, if the network contains a loop formed of voltage sources, then the voltage values must add up to zero in order to obey KVL. Subsequently, we will consider circuits that do not contain loops of voltage sources.

We assume that the above four circuit elements are *ideal*, meaning that their behaviour is determined by the following characteristics (see Figure 2):

- The current-voltage (i - v) characteristic of a voltage source satisfies $v = v_0$ for some constant voltage value v_0 , regardless of the current i .
- A resistor follows Ohm’s law, i.e. its i - v characteristic is $i = gv$, where g is the conductance ($g = 1/r$ where r is the resistance).
- The i - v characteristic of a diode satisfies $i = 0$ for $v < 0$, and $v = 0$ for $i > 0$.
- A voltage-controlled voltage source (VCVS) has four terminals: two input terminals whose voltage we denote v_{in} , and two output terminals whose voltage we denote v_{out} . It satisfies the relationship $v_{\text{out}} = Av_{\text{in}}$, where $A > 0$ is the ‘gain’ (or ‘amplification factor’).

Under these assumptions, nonlinear resistive networks are universal function approximators in the following sense.

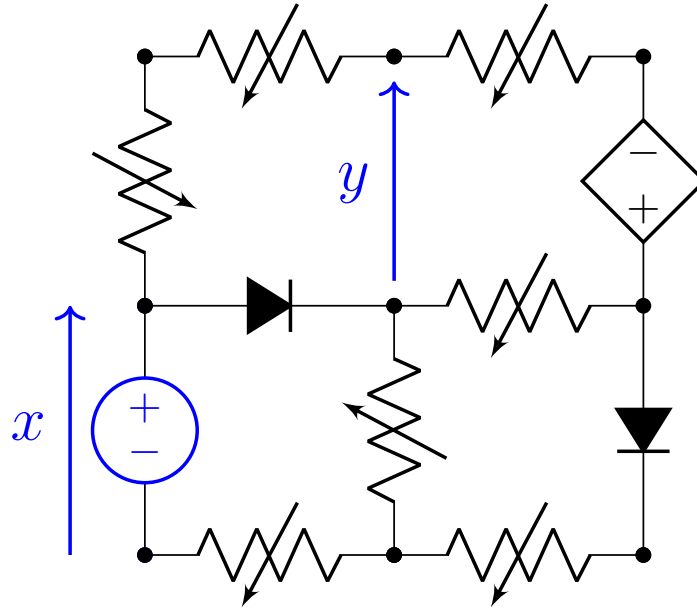


Figure 1. A **nonlinear resistive network** composed of variable resistors, voltage sources, diodes and voltage-controlled voltage sources (VCVS). Voltage sources are used as inputs (x) and voltages across pairs of ‘output nodes’ are used as outputs (y). Variable resistors represent the trainable weights, diodes introduce nonlinearities, and the VCVSs are used for amplification. Such electrical networks are universal function approximators (Theorem 1). Note: for simplicity, the input terminals of the VCVS are not represented on the figure ; only its output terminals are displayed.

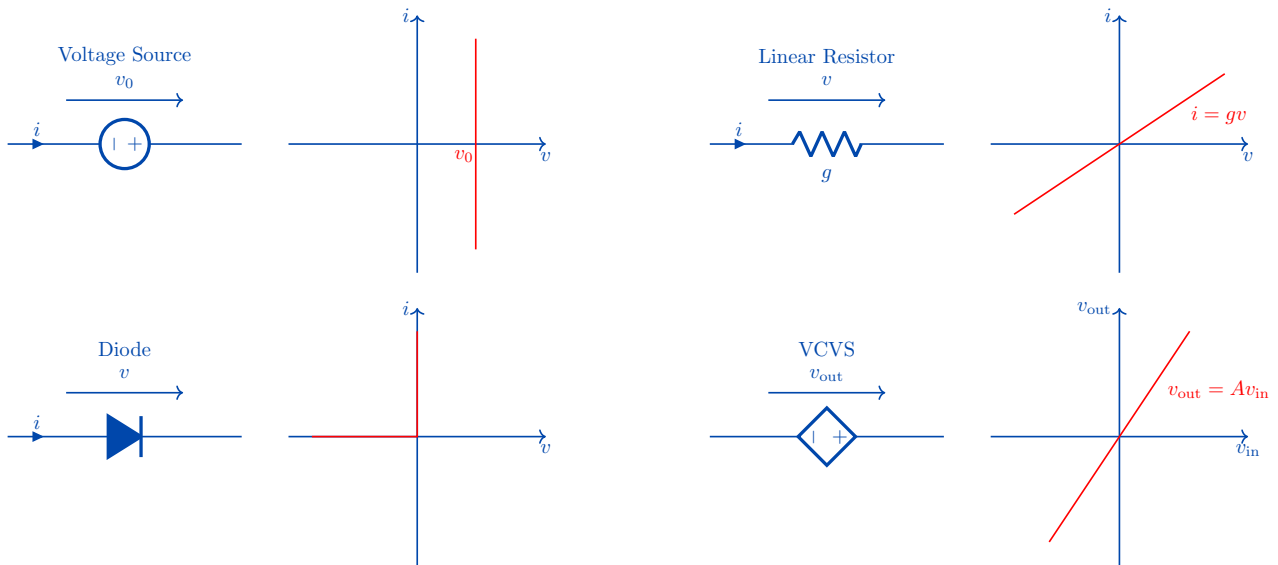


Figure 2. **Current-voltage (i-v) characteristics of ideal elements.** A linear resistor is characterized by Ohm’s law: $i = gv$, where g is the conductance of the resistor ($g = 1/r$ where r is the resistance). An ideal diode is characterized by $i = 0$ for $v \leq 0$ (“off state”, behaving like an open switch), and $v = 0$ for $i > 0$ (“on state”, behaving like a closed switch). An ideal voltage source is characterized by $v = v_0$ for some constant voltage v_0 . Finally, a voltage-controlled voltage source (VCVS) has four terminals – two terminals that form an input voltage v_{in} and two terminals that form an output voltage v_{out} – and is characterized by the relationship $v_{out} = Av_{in}$, where $A > 0$ is the amplification factor, or gain. Note: for simplicity, the input terminals of the VCVS are not represented on the figure ; only its output terminals are represented.

Theorem 1 (A universal approximation theorem for nonlinear resistive networks). *Given any continuous function $f : \mathbb{R}^p \rightarrow \mathbb{R}^q$, and given any compact subset $C \subset \mathbb{R}^p$ and any $\epsilon > 0$, there exists a nonlinear resistive network with p input voltage sources and q output branches such that, under the above assumptions of ideality, the function $F : \mathbb{R}^p \rightarrow \mathbb{R}^q$ that the nonlinear resistive network implements (i.e., the mapping between the inputs and outputs to the network) satisfies*

$$\|F(x) - f(x)\| \leq \epsilon, \quad \forall x \in C. \quad (1)$$

The main aim of the next section is to prove Theorem 1.

3. Universal approximation through neural network approximation

To prove Theorem 1, we show that nonlinear resistive networks can approximate ReLU neural networks to any desired accuracy. Since ReLU neural networks are universal approximators, it follows that nonlinear resistive networks are universal approximators, too.

We proceed in three steps. First, we recall the definition of a ReLU neural network (Section 3.1) and their universal approximation property (Theorem 2). Then, we present a layered nonlinear resistive network model similar to the one proposed by Kendall et al. (2020) that we call ‘deep resistive network’, or DRN (Section 3.2). Under the assumptions of Section 2, we derive the equations characterizing the steady state of a DRN (Lemma 3). Finally, using Lemma 3, we prove that any ReLU neural network can be approximated by a DRN (Theorem 5 in Section 3.3). Combining everything, our main Theorem 1 is a consequence of Theorem 2 and Theorem 5. Proofs of the Lemmas and Theorems are provided in Appendix A.

3.1. ReLU neural network

A neural network processes an input vector x through several transformation stages to produce an output vector. We consider specifically the multi-layer perceptron (MLP) architecture with the rectified linear unit (ReLU) activation function. We refer to this model as the ‘ReLU neural network’ (ReLU NN).

A ReLU NN consists of L stages of transformation, called ‘layers’. The input vector is processed sequentially from the input layer (of index $\ell = 0$) to the output layer (of index $\ell = L$), through the hidden layers ($1 \leq \ell \leq L - 1$). Each layer ℓ has a dimension M_ℓ , a.k.a the number of ‘units’ of the layer. Denoting $s_k^{(\ell)}$ the state of the k -th unit of layer ℓ , the equations defining the network’s state are the following:

1. Input layer:

$$s_k^{(0)} := x_k, \quad 1 \leq k \leq M_0, \quad (2)$$

where $x = (x_1, \dots, x_{M_0})$ is the input vector.

2. Hidden layers:

$$s_k^{(\ell)} := \max \left(0, \sum_{j=1}^{M_{\ell-1}} w_{jk}^{(\ell)} s_j^{(\ell-1)} + b_k^{(\ell)} \right), \quad (3)$$

for every (ℓ, k) such that $1 \leq \ell \leq L - 1$ and $1 \leq k \leq M_\ell$.

3. Output layer:

$$s_k^{(L)} := \sum_{j=1}^{M_{L-1}} w_{jk}^{(L)} s_j^{(L-1)} + b_k^{(L)}, \quad 1 \leq k \leq M_L. \quad (4)$$

In these equations, the units’ transformations are parameterized by the ‘weights’ $w_{jk}^{(\ell)}$ and ‘biases’ $b_k^{(\ell)}$. The $\max(0, \cdot)$ function is called the ‘ReLU’ nonlinear activation function (Glorot et al., 2011). The network thus implements a function $G : \mathbb{R}^{M_0} \rightarrow \mathbb{R}^{M_L}$ mapping input x to output $s^{(L)}$.

Theorem 2 (ReLU NNs are universal function approximators). *ReLU NNs can approximate any continuous function on a compact subset. Specifically, for any continuous function $f : \mathbb{R}^p \rightarrow \mathbb{R}^q$, compact subset $C \subset \mathbb{R}^p$, and $\epsilon > 0$, there exists a ReLU NN with $L = 2$ layers, $M_0 = p$ input units, and $M_2 = q$ output units such that:*

$$\|G(x) - f(x)\| \leq \epsilon, \quad \forall x \in C, \quad (5)$$

where G is the function implemented by the ReLU NN.

This result was first proved in Leshno et al. (1993) – see also Yarotsky (2017). We will use this result to prove our Theorem 1.

3.2. Deep resistive network

Next, we present a nonlinear resistive network model similar to the one of Kendall et al. (2020) that takes inspiration from the layered architecture of neural networks. We call it ‘deep resistive network’, or DRN. Our goal will be to prove that DRNs can approximate ReLU NNs to arbitrary accuracy.

In a DRN, the circuit elements - voltage sources, resistors and diodes - are assembled to form a layered network. A DRN is depicted in Figure 3 and defined as follows. First of all, we choose a reference node called ‘ground’. We denote L the number of layers in the DRN, and for each ℓ such that $0 \leq \ell \leq L$, we denote N_ℓ the number of nodes in layer ℓ . We choose $N_0 = 2p + 2$ input nodes and $N_L = q$ output

nodes. We also call each node a ‘unit’ by analogy with the units of a neural network. We denote $v_k^{(\ell)}$ the electrical potential of the k -th node of layer ℓ , which we may think of as the unit’s activation. Pairs of nodes from two consecutive layers are interconnected by (variable) resistors, i.e. the ‘trainable weights’. We denote $g_{jk}^{(\ell)}$ the conductance of the resistor between the j -th node of layer $\ell - 1$ and the k -th node of layer ℓ . The layer of index $\ell = 0$ is the ‘input layer’, whose units are connected to ground by VCVS’s with the same gain $A^{(0)} > 0$. Moreover, there are p voltage sources that play the role of input variables and serve as input voltages to the $2p$ VCVS’s. Given an input vector $x = (x_1, \dots, x_p)$, we set the p input voltage sources to x_1, \dots, x_p , so that the input nodes (VCVS output voltages) have electrical potentials

$$v_{2k}^{(0)} := +A^{(0)}x_k, \quad v_{2k+1}^{(0)} := -A^{(0)}x_k, \quad 1 \leq k \leq p. \quad (6)$$

The units of intermediate (‘hidden’) layers ($1 \leq \ell \leq L - 1$) of the network are nonlinear: for each hidden unit, a diode is placed between the unit’s node and ground, which can be oriented in either of the two directions. For the units of even index k , the diode points from the unit’s node to ground, so the unit’s electrical potential is non-negative: when it reaches 0, current flows through the diode from ground to the unit’s node so as to maintain the unit’s electrical potential at zero; we call such a unit an *excitatory unit*. Conversely, for the units of odd index k , the diode points from ground to the unit’s node, so the unit’s electrical potential is non-positive: when it reaches 0, the extra current sinks to ground through the diode; we call it an *inhibitory unit*. Thus, half of the hidden units are excitatory and the other half are inhibitory. Output units are linear, meaning that no diode is used for the output units. Finally, each hidden and output unit $v_k^{(\ell)}$ is also linked to ground by a resistor whose conductance is denoted $g_k^{(\ell)}$. In addition, each of the input and hidden layers contains a pair of ‘bias units’ that are connected to ground by voltage sources of fixed voltages:

$$v_0^{(\ell)} := +A^{(\ell)}, \quad v_1^{(\ell)} := -A^{(\ell)}, \quad 0 \leq \ell \leq L - 1, \quad (7)$$

where $A^{(\ell)} > 0$ a layer-wise scalar – the ‘gain’ of layer ℓ .

Under the assumptions of ideality of the elements (Section 2), the steady state of the DRN – the configuration of branch voltages and branch currents that satisfies all the branch equations, as well as KCL and KVL – is determined by the following set of equations.

Lemma 3 (Equations of a DRN). *For every (ℓ, k) such that*

$1 \leq \ell \leq L - 1$ and $2 \leq k \leq N_\ell$, the equations for $v_k^{(\ell)}$ is

$$p_k^{(\ell)} = \frac{\sum_{j=1}^{N_{\ell-1}} g_{jk}^{(\ell)} v_j^{(\ell-1)} + \sum_{j=1}^{N_{\ell+1}} g_{kj}^{(\ell+1)} v_j^{(\ell+1)}}{g_k^{(\ell)} + \sum_{j=1}^{N_{\ell-1}} g_{jk}^{(\ell)} + \sum_{j=1}^{N_{\ell+1}} g_{kj}^{(\ell+1)}} \quad (8)$$

$$v_k^{(\ell)} = \begin{cases} \max\left(0, p_k^{(\ell)}\right) & \text{if } k \text{ is even (excitatory unit),} \\ \min\left(0, p_k^{(\ell)}\right) & \text{if } k \text{ is odd (inhibitory unit).} \end{cases} \quad (9)$$

As for the equation of the output unit $v_k^{(L)}$,

$$v_k^{(L)} = \frac{\sum_{j=1}^{N_{L-1}} g_{jk}^{(L)} v_j^{(L-1)}}{g_k^{(L)} + \sum_{j=1}^{N_{L-1}} g_{jk}^{(L)}}, \quad 1 \leq k \leq q. \quad (10)$$

A few remarks are in order. First, the equations characterizing the steady state of a DRN share similarities with those of a ReLU NN (Eq. (2)-(4)): these equations involve a weighted sum of the neighboring units’ activities (electrical potentials), and the function $\max(0, \cdot)$ is the ‘ReLU’ nonlinear activation function.

However, the equations of a DRN and a ReLU NN are not identical: a DRN is not a ReLU NN. One difference is that, in a DRN, the units of a given layer ℓ receive signals not just from the previous layer $\ell - 1$ but also from the next layer $\ell + 1$, in other words signals flow in both the forward and backward directions.

Another difference is that these signals are normalized by the sum of the weights (total conductance) $g_k^{(\ell)} + \sum_{j=1}^{N_{\ell-1}} g_{jk}^{(\ell)} + \sum_{j=1}^{N_{\ell+1}} g_{kj}^{(\ell+1)}$. This results in the following *layer-wise maximum principle*, summarized in the Lemma below,

Lemma 4 (A maximum principle for DRNs). *For every ℓ such that $0 \leq \ell \leq L$, denote the maximum amplitude of electrical potential in layer ℓ as*

$$Z^{(\ell)} := \max_{1 \leq k \leq N_\ell} |v_k^{(\ell)}|. \quad (11)$$

Then we have

$$Z^{(\ell)} \leq Z^{(\ell-1)}, \quad 1 \leq \ell \leq L. \quad (12)$$

In particular, the electrical potentials of the units are bounded by the electrical potentials of input units:

$$|v_k^{(\ell)}| \leq \max_{1 \leq j \leq N_0} |v_j^{(0)}|, \quad 0 \leq \ell \leq L, \quad 1 \leq k \leq N_\ell. \quad (13)$$

As a consequence of the above lemma, the signal strengths decrease as the index of the layer (ℓ) increases. This is the reason why voltage-controlled voltage sources (VCVS) are used: they amplify the input signals by a gain $A^{(0)}$ to compensate for the decay in amplitude and ensure that the signals at the output layer do not vanish.

Another difference between DRNs and ReLU NNs is that the ‘weights’ of a DRN are non-negative - a conductance is non-negative - meaning $g_{jk}^{(\ell)} \geq 0$. This is the reason why, in addition to excitatory units, we also use inhibitory units, so the network can communicate ‘negative signals’ too. This is also the reason why we have doubled the number of input VCVS’s in the input layer (two VCVS’s for each input voltage source).

3.3. Approximating a ReLU neural network with a deep resistive network

Given a ReLU NN, we show that we can build a DRN (parametrized by a number $\gamma > 0$) that approximates the ReLU NN. To this end, let L be the number of layers of the ReLU NN, and M_ℓ the number of units in layer ℓ , for $1 \leq \ell \leq L$. We denote $w_{jk}^{(\ell)}$ and $b_k^{(\ell)}$ the weights and biases. Given an input vector $x = (x_1, \dots, x_{M_0})$, we also denote $s_k^{(\ell)}$ the state of the k -th unit in layer ℓ of the ReLU NN.

We build the DRN as follows. First we define its architecture. The DRN consists of L layers and contains $N_\ell := 2M_\ell + 2$ units in layer ℓ for $1 \leq \ell \leq L - 1$ and $N_L := M_L$ units in layer L . It remains to choose the values of the conductances ($g_{jk}^{(\ell)}$) and the amplification factors ($A^{(\ell)}$) for input and hidden layers. First we define for convenience $w_{0k}^{(\ell)} := b_k^{(\ell)}$. We also introduce $\gamma > 0$ a dimensionless number ; later we will let $\gamma \rightarrow 0$ to establish the equivalence of the DRN and the ReLU NN. For every triplet (ℓ, j, k) such that $1 \leq \ell \leq L - 1$, $0 \leq j \leq M_{\ell-1}$ and $1 \leq k \leq M_\ell$, we define

$$g_{2j,2k}^{(\ell)} := \max(0, \gamma^\ell w_{jk}^{(\ell)}), \quad (14)$$

$$g_{2j,2k+1}^{(\ell)} := \max(0, -\gamma^\ell w_{jk}^{(\ell)}), \quad (15)$$

$$g_{2j+1,2k}^{(\ell)} := \max(0, -\gamma^\ell w_{jk}^{(\ell)}), \quad (16)$$

$$g_{2j+1,2k+1}^{(\ell)} := \max(0, \gamma^\ell w_{jk}^{(\ell)}). \quad (17)$$

Furthermore, for every (j, k) such that $0 \leq j \leq M_{L-1}$ and $1 \leq k \leq M_L$, we define

$$g_{2j,k}^{(L)} := \max(0, \gamma^L w_{jk}^{(L)}), \quad (18)$$

$$g_{2j+1,k}^{(L)} := \max(0, -\gamma^L w_{jk}^{(L)}). \quad (19)$$

The conductances thus defined are all non-negative. Next, for every ℓ such that $1 \leq \ell \leq L$, we define

$$a^{(\ell)} := \max_{1 \leq k \leq M_\ell} \left(\sum_{j=0}^{M_{\ell-1}} |w_{jk}^{(\ell)}| \right), \quad (20)$$

and for every (ℓ, k) such that $1 \leq \ell \leq L$ and $1 \leq k \leq M_\ell$, we define

$$g_{2k}^{(\ell)} := g_{2k+1}^{(\ell)} := \gamma^\ell \left(a^{(\ell)} - \sum_{j=0}^{M_{\ell-1}} |w_{jk}^{(\ell)}| \right). \quad (21)$$

The conductances $g_{2k}^{(\ell)}$ and $g_{2k+1}^{(\ell)}$ are also non-negative, by definition of $a^{(\ell)}$. Finally, we define the amplification factors for input and hidden layers

$$A^{(\ell)} := a^{(\ell+1)} \times a^{(\ell+2)} \times \dots \times a^{(L)}, \quad 0 \leq \ell \leq L - 1. \quad (22)$$

Theorem 5 (Approximation of a ReLU NN with a DRN). *Suppose that, given an input signal $x = (x_1, x_2, \dots, x_{M_0})$, we set the input voltage sources to*

$$v_{2k}^{(0)} := A^{(0)} x_k, \quad v_{2k+1}^{(0)} := -A^{(0)} x_k, \quad 1 \leq k \leq M_0. \quad (23)$$

Denote $\|x\|_\infty := \max_{1 \leq k \leq M_0} |x_k|$. Then, in the limit $\gamma \rightarrow 0$, for every (ℓ, k) such that $1 \leq \ell \leq L - 1$ and $1 \leq k \leq M_\ell$, we have:

$$v_{2k}^{(\ell)} = A^{(\ell)} s_k^{(\ell)} + O(\gamma \|x\|_\infty), \quad (24)$$

$$v_{2k+1}^{(\ell)} = -A^{(\ell)} s_k^{(\ell)} + O(\gamma \|x\|_\infty), \quad (25)$$

$$v_k^{(L)} = s_k^{(L)} + O(\gamma \|x\|_\infty), \quad 1 \leq k \leq M_L. \quad (26)$$

Namely, when $\gamma \rightarrow 0$, the states of the excitatory units of the DRN tend to the states of the units of the ReLU NN rescaled by $A^{(\ell)}$. In particular, the states of output units of the DRN are equal to those of the ReLU NN, up to $O(\gamma \|x\|_\infty)$. In other words, the function implemented by the DRN approximates the function implemented by the ReLU NN.

Using a symmetry argument, one can prove that the DRN thus built has the property that $v_{2k+1}^{(\ell)} = -v_{2k}^{(\ell)}$ for every (ℓ, k) . Although it might seem wasteful and redundant to have two units encode the same piece of information, we recall that doubling the number of units per layer (using excitatory and inhibitory units) is also what allows us to overcome the constraint of non-negative conductances in resistive networks.

Technically, the reason why the DRN behaves essentially like a feedforward network (ReLU NN) is that we scale the conductances of each layer ℓ by γ^ℓ , using $\gamma \ll 1$. While this trick is mathematically convenient to derive Theorem 5, it would also likely be impractical for deep networks as the range of conductance values will span over multiple orders of magnitude, proportional to the number of layers L . It is noteworthy, however, that ReLU NNs with a single hidden layer ($L = 2$) are also universal approximators (Theorem 2). The DRNs corresponding to such ReLU NNs have a single hidden layer, therefore the range spanned by their conductance values is smaller.

4. Simulations

In this section, we illustrate the expressivity of nonlinear resistive networks in simulations. We show that DRNs can

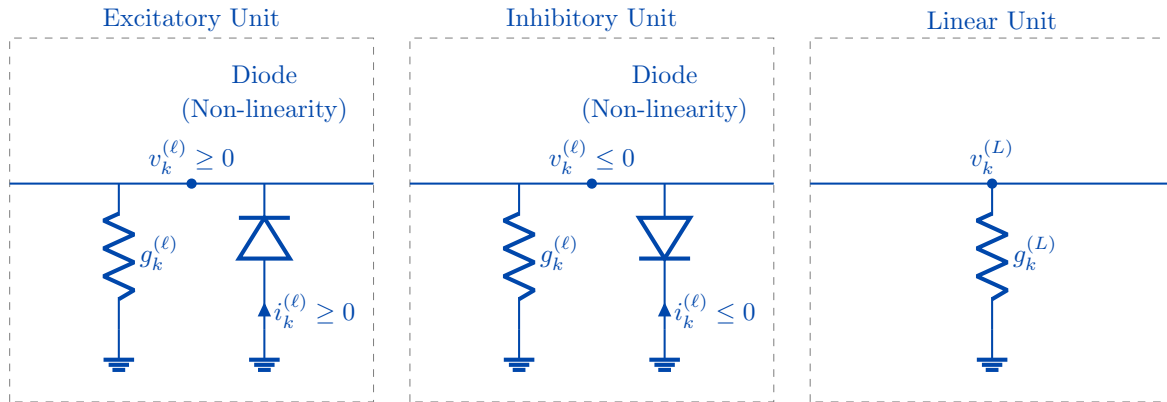
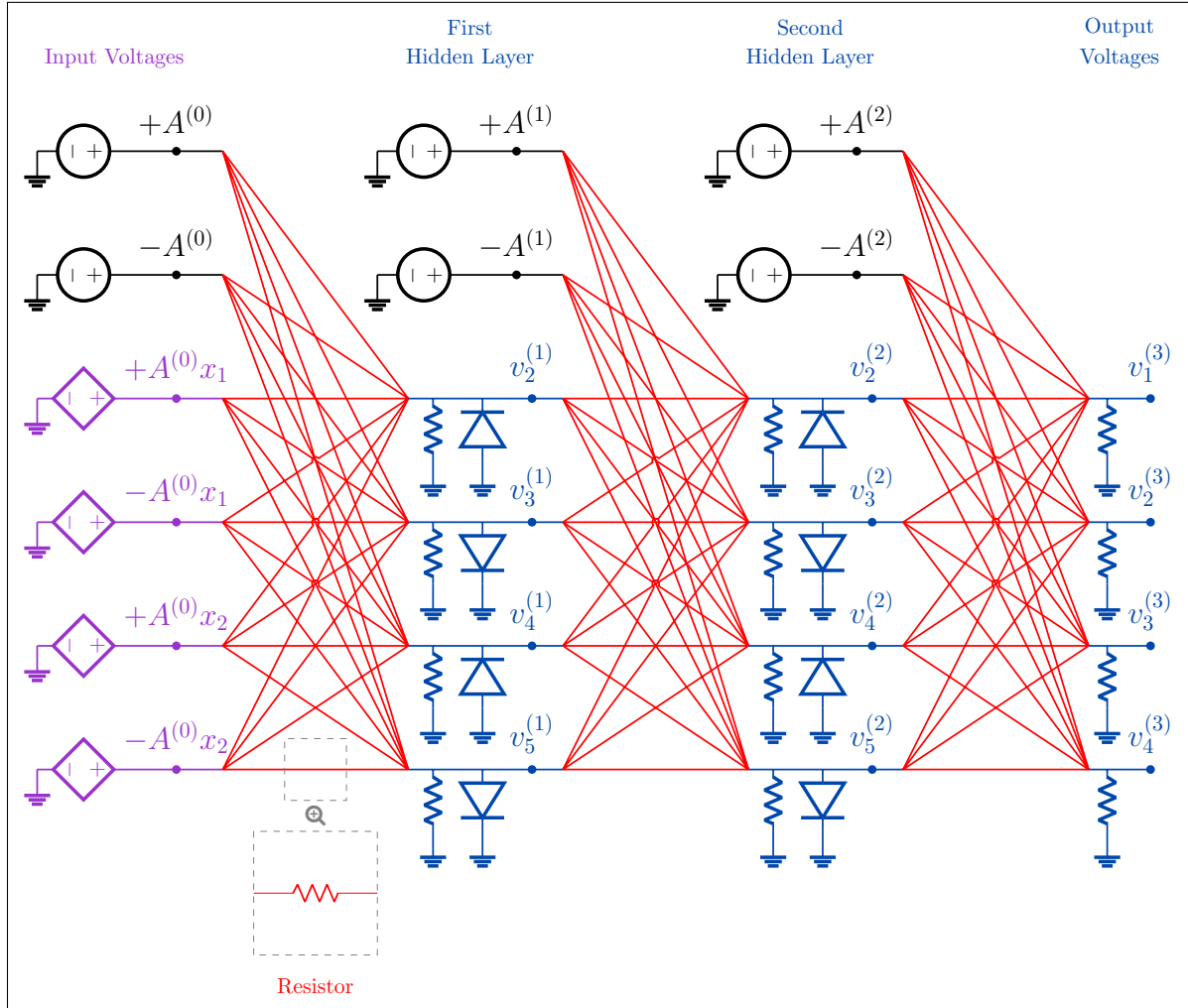


Figure 3. A deep resistive network (DRN). **Top.** A DRN consists of ‘units’ (excitatory, inhibitory or linear, shown in blue) interconnected by variable resistors (in red). Input voltages (x_1 and x_2) are applied to the network via voltage sources (not shown in the figure for readability) and are amplified using VCVS’s to generate the electrical potentials $+A^{(0)}x_1$, $-A^{(0)}x_1$, $+A^{(0)}x_2$ and $-A^{(0)}x_2$ at designated ‘input nodes’ (in purple). The model’s prediction is read from a set of output nodes ($v_1^{(3)}$, $v_2^{(3)}$, $v_3^{(3)}$ and $v_4^{(3)}$). Additionally, each layer includes two voltage sources serving as ‘biases’ (shown in black). **Bottom.** Each unit is connected to ground through a resistor. Nonlinear units are constructed by placing a diode between the unit’s node and ground. Depending on the orientation of the diode, nonlinear units can be either ‘excitatory’ or ‘inhibitory’. Units without a diode are called ‘linear’ units.

be trained to achieve comparable performance to ReLU NNs on the MNIST, Kuzushiji-MNIST and Fashion-MNIST datasets. We train DRNs with one, two and three hidden layers, denoted as DRN-1H, DRN-2H and DRN-3H, respectively. We compare their performances to their corresponding ReLU NNs. Each DRN has 1568 input units ($2 \times 28 \times 28$), 10 output units corresponding to the ten classes of the MNIST dataset, and 1024 units per hidden layer. Each ReLU NN has 784 input units (28×28), 10 output units and 512 units per hidden layer. We use the algorithm of Scellier (2024a) to compute the DRN steady states necessary to extract the weight (conductance) gradients to perform stochastic gradient descent. A full description of the models, algorithms and hyperparameters used for training are provided in Appendix D. Our code to reproduce the results is available at <https://github.com/rain-neuromorphics/energy-based-learning>.

Table 1. Comparison of deep resistive networks (DRNs) and their equivalent-size ReLU neural networks (ReLU NNs). We train DRNs and ReLU NNs with one, two and three hidden layers on MNIST, F-MNIST and K-MNIST. For each experiment, we perform five runs and we report the mean values and std values of the test error rates (in %). See Appendix D for the architectural details of the DRN and ReLU NN models, as well as the algorithms used to train them.

DATASET	NETWORK MODEL	TEST ERROR (%)
MNIST	DRN-1H	1.51 ± 0.04
	ReLU NN-1H	1.67 ± 0.03
	DRN-2H	1.46 ± 0.05
	ReLU NN-2H	1.34 ± 0.01
	DRN-3H	1.47 ± 0.08
	ReLU NN-3H	1.48 ± 0.03
KUZUSHIJI MNIST	DRN-1H	7.67 ± 0.13
	ReLU NN-1H	8.83 ± 0.11
	DRN-2H	8.27 ± 0.02
	ReLU NN-2H	8.14 ± 0.13
	DRN-3H	8.39 ± 0.24
	ReLU NN-3H	7.99 ± 0.23
FASHION MNIST	DRN-1H	10.31 ± 0.05
	ReLU NN-1H	10.20 ± 0.11
	DRN-2H	9.88 ± 0.11
	ReLU NN-2H	9.42 ± 0.22
	DRN-3H	9.79 ± 0.25
	ReLU NN-3H	9.55 ± 0.14

As discussed earlier, one limiting assumption in our mathematical derivation of Theorem 5 is the requirement to scale the weights (conductances) of layer ℓ by a factor γ^ℓ , where $\gamma \ll 1$. Interestingly, however, our simulation results suggest that this scaling is not necessary in practice. In Table 2, we report for each DRN model and for each layer ℓ the

mean and standard deviation of the conductance matrix $g^{(\ell)}$ after training. As one can see, the difference in conductance values across layers are not significant, demonstrating that conductance matrices do not actually need to span over multiple orders of magnitude.

Table 2. Conductance values of the DRN models after training (DRN-1H, DRN-2H and DRN-3H). We report the mean, standard deviation and maximum values of the conductance matrices ($g^{(k)}$) for each of the three DRN models.

		$g^{(1)}$	$g^{(2)}$	$g^{(3)}$	$g^{(4)}$
DRN-1H	MEAN	0.0077	0.0091		
	STD	0.0102	0.0327		
	MAX	0.2069	0.3295		
DRN-2H	MEAN	0.0071	0.0074	0.0024	
	STD	0.0082	0.0102	0.0249	
	MAX	0.0996	0.1459	0.4897	
DRN-3H	MEAN	0.0076	0.0079	0.0053	0.0034
	STD	0.0086	0.0113	0.0124	0.0230
	MAX	0.1276	0.4104	0.8345	0.4125

5. Discussion

Since the seminal work of Cybenko (1989), the concept of universal function approximation has been extensively studied in the context of neural networks (NNs). However, the computational capabilities of analog physical systems that are not isomorphic to NNs remain largely unexplored (see e.g. Stern & Murugan (2023) for a review). In this study, we have examined the expressive power of resistor networks, which use voltage sources as inputs and variable resistors as trainable weights. These networks have recently garnered interest due to their ability to be trained by gradient descent using local learning rules (Kendall et al., 2020; Anisetti et al., 2024), and practical implementations of such self-learning resistor networks have already been demonstrated (Dillavou et al., 2022; 2024). Our study advances our understanding of the computational properties of these resistor networks, and further highlights their potential. We have shown that, under suitable assumptions, resistor networks equipped with diodes and voltage-controlled voltage sources (VCVS) – referred to as nonlinear resistive networks – can approximate any continuous function. Central to our proof is the demonstration that a subclass of these electrical networks – so-called ‘deep resistive networks’ (DRNs) – can approximate arbitrary ReLU NNs with any desired precision. Our result thus offers a method for translating a ReLU NN into an approximately equivalent DRN.

Nonetheless, our theoretical results rely on several assumptions, some of which are impractical. First, to derive our results, we have assumed ideal diodes, but real-world diodes

deviate significantly from our idealized model. Future works could attempt to adapt our approach to networks with more realistic current-voltage (i - v) characteristics, e.g. by adapting the steps from Eq. (29) to Eq. (32) in our derivation (Appendix A). Second, our construction uses VCVS with very large gains ($A^{(0)} \gg 1$) to amplify the DRN’s input signals, which would be impractical in an actual circuit. A solution proposed by Kendall et al. (2020) is to use layer-wise ‘bidirectional amplifiers’ with smaller gains, as a replacement for the input VCVS - see Appendix C for details. Third, we have assumed that the conductances of the variable resistors can be adjusted to arbitrary non-negative values - arbitrarily large or arbitrarily small - but in practice, real-world memristors have quantized conductance values and operate within a finite range. Fourth, our model is deterministic, whereas real-world analog electrical networks are inherently noisy. Despite these assumptions, our universal approximation theorem represents the first theoretical result of its kind for analog resistor networks, and we believe that it can serve as a basis for deriving more practical theorems requiring fewer or more realistic assumptions.

We also note that nonlinear resistive networks are closely related to continuous Hopfield networks (CHNs) (Hopfield, 1984) - for a comparison, see Scellier (2024a, Appendix E). In particular, the idea of rescaling the weights layer-wise, so the DRN behaves approximately as a ReLU NN, is reminiscent of the work by Xie & Seung (2003) where it is shown that layered NNs can be approximated by layered CHNs using a similar technique. The similarity between nonlinear resistive networks and CHNs is appealing, particularly as recent studies have shown through simulations that CHNs can be effectively trained using equilibrium propagation on datasets like CIFAR10, CIFAR100, and ImageNet 32×32 , yielding promising results (Laborieux et al., 2021; Laborieux & Zenke, 2022; Scellier et al., 2024).

Acknowledgements

The authors thank Jack Kendall, Maxence Ernoult, Mohammed Fouda, Suhas Kumar, Vidyesh Anisetti, Andrea Liu, Axel Laborieux and Tim De Ryck for discussions.

References

- Altman, L. E., Stern, M., Liu, A. J., and Durian, D. J. Experimental demonstration of coupled learning in elastic networks. *Physical Review Applied*, 22(2):024053, 2024.
- Anisetti, V. R., Kandala, A., Scellier, B., and Schwarz, J. Frequency propagation: Multimechanism learning in nonlinear physical networks. *Neural Computation*, pp. 1–25, 2024.
- Clanuwat, T., Bober-Irizar, M., Kitamoto, A., Lamb, A., Yamamoto, K., and Ha, D. Deep learning for classical japanese literature. *arXiv preprint arXiv:1812.01718*, 2018.
- Cybenko, G. Approximation by superpositions of a sigmoidal function. *Mathematics of control, signals and systems*, 2(4):303–314, 1989.
- Dillavou, S., Stern, M., Liu, A. J., and Durian, D. J. Demonstration of decentralized physics-driven learning. *Physical Review Applied*, 18(1):014040, 2022.
- Dillavou, S., Beyer, B. D., Stern, M., Liu, A. J., Miskin, M. Z., and Durian, D. J. Machine learning without a processor: Emergent learning in a nonlinear analog network. *Proceedings of the National Academy of Sciences*, 121(28):e2319718121, 2024.
- Glorot, X., Bordes, A., and Bengio, Y. Deep sparse rectifier neural networks. In *Proceedings of the fourteenth international conference on artificial intelligence and statistics*, pp. 315–323, 2011.
- Harris, J., Koch, C., Luo, J., and Wyatt, J. Resistive fuses: Analog hardware for detecting discontinuities in early vision. In *Analog VLSI implementation of neural systems*, pp. 27–55. Springer, 1989.
- Hermans, M., Burm, M., Van Vaerenbergh, T., Dambre, J., and Bienstman, P. Trainable hardware for dynamical computing using error backpropagation through physical media. *Nature communications*, 6(1):6729, 2015.
- Hopfield, J. J. Neurons with graded response have collective computational properties like those of two-state neurons. *Proceedings of the national academy of sciences*, 81(10):3088–3092, 1984.
- Kendall, J., Pantone, R., Manickavasagam, K., Bengio, Y., and Scellier, B. Training end-to-end analog neural networks with equilibrium propagation. *arXiv preprint arXiv:2006.01981*, 2020.
- Kiraz, F. Z., Pham, D.-K. G., and Desgreys, P. Impacts of feedback current value and learning rate on equilibrium propagation performance. In *2022 20th IEEE International NEWCAS Conference (NEWCAS)*, pp. 519–523. IEEE, 2022.
- Laborieux, A. and Zenke, F. Holomorphic equilibrium propagation computes exact gradients through finite size oscillations. *Advances in Neural Information Processing Systems*, 35:12950–12963, 2022.
- Laborieux, A., Ernoult, M., Scellier, B., Bengio, Y., Grollier, J., and Querlioz, D. Scaling equilibrium propagation to deep convnets by drastically reducing its gradient estimator bias. *Frontiers in neuroscience*, 15:129, 2021.

- Laydevant, J., Marković, D., and Grollier, J. Training an ising machine with equilibrium propagation. *Nature Communications*, 15(1):3671, 2024.
- LeCun, Y., Bottou, L., Bengio, Y., and Haffner, P. Gradient-based learning applied to document recognition. *Proceedings of the IEEE*, 86(11):2278–2324, 1998.
- Leshno, M., Lin, V. Y., Pinkus, A., and Schocken, S. Multilayer feedforward networks with a nonpolynomial activation function can approximate any function. *Neural networks*, 6(6):861–867, 1993.
- Li, B., Xia, L., Gu, P., Wang, Y., and Yang, H. Merging the interface: Power, area and accuracy co-optimization for rram crossbar-based mixed-signal computing system. In *Proceedings of the 52nd annual design automation conference*, pp. 1–6, 2015.
- Lopez-Pastor, V. and Marquardt, F. Self-learning machines based on hamiltonian echo backpropagation. *Physical Review X*, 13(3):031020, 2023.
- Massar, S. and Mognetti, B. M. Equilibrium propagation: the quantum and the thermal cases. *arXiv preprint arXiv:2405.08467*, 2024.
- Millar, W. Cxvi. some general theorems for non-linear systems possessing resistance. *The London, Edinburgh, and Dublin Philosophical Magazine and Journal of Science*, 42(333):1150–1160, 1951.
- Momeni, A., Rahmani, B., Malléjac, M., Del Hougne, P., and Fleury, R. Backpropagation-free training of deep physical neural networks. *Science*, 382(6676):1297–1303, 2023.
- Momeni, A., Rahmani, B., Scellier, B., Wright, L. G., McMahon, P. L., Wanjura, C. C., Li, Y., Skalli, A., Berloff, N. G., Onodera, T., et al. Training of physical neural networks. *arXiv preprint arXiv:2406.03372*, 2024.
- Oh, S., An, J., Cho, S., Yoon, R., and Min, K.-S. Memristor crossbar circuits implementing equilibrium propagation for on-device learning. *Micromachines*, 14(7):1367, 2023.
- Paszke, A., Gross, S., Chintala, S., Chanan, G., Yang, E., DeVito, Z., Lin, Z., Desmaison, A., Antiga, L., and Lerer, A. Automatic differentiation in pytorch. 2017.
- Scellier, B. *A deep learning theory for neural networks grounded in physics*. PhD thesis, Université de Montréal, 2021.
- Scellier, B. A fast algorithm to simulate nonlinear resistive networks. In *Forty-first International Conference on Machine Learning*. PMLR, 2024a.
- Scellier, B. Quantum equilibrium propagation: Gradient-descent training of quantum systems. *arXiv preprint arXiv:2406.00879*, 2024b.
- Scellier, B. and Bengio, Y. Equilibrium propagation: Bridging the gap between energy-based models and backpropagation. *Frontiers in computational neuroscience*, 11:24, 2017.
- Scellier, B., Mishra, S., Bengio, Y., and Ollivier, Y. Agnostic physics-driven deep learning. *arXiv preprint arXiv:2205.15021*, 2022.
- Scellier, B., Ernoult, M., Kendall, J., and Kumar, S. Energy-based learning algorithms for analog computing: a comparative study. *Advances in Neural Information Processing Systems*, 36, 2024.
- Stern, M. and Murugan, A. Learning without neurons in physical systems. *Annual Review of Condensed Matter Physics*, 14:417–441, 2023.
- Stern, M., Hexner, D., Rocks, J. W., and Liu, A. J. Supervised learning in physical networks: From machine learning to learning machines. *Physical Review X*, 11(2):021045, 2021.
- Stern, M., Dillavou, S., Miskin, M. Z., Durian, D. J., and Liu, A. J. Physical learning beyond the quasistatic limit. *Physical Review Research*, 4(2):L022037, 2022.
- Stern, M., Dillavou, S., Jayaraman, D., Durian, D. J., and Liu, A. J. Training self-learning circuits for power-efficient solutions. *APL Machine Learning*, 2(1), 2024a.
- Stern, M., Liu, A. J., and Balasubramanian, V. Physical effects of learning. *Physical Review E*, 109(2):024311, 2024b.
- Wang, Q., Wanjura, C., and Marquardt, F. Training coupled phase oscillators as a neuromorphic platform using equilibrium propagation. *Neuromorphic Computing and Engineering*, 2024.
- Wanjura, C. C. and Marquardt, F. Fully nonlinear neuromorphic computing with linear wave scattering. *Nature Physics*, pp. 1–7, 2024a.
- Wanjura, C. C. and Marquardt, F. Quantum equilibrium propagation for efficient training of quantum systems based on onsager reciprocity. *arXiv e-prints*, pp. arXiv–2406, 2024b.
- Wafsa, M., Garcia-Ortiz, A., and Sassatelli, G. Energy-based analog neural network framework. *Frontiers in Computational Neuroscience*, 17:1114651, 2023.

- Wright, L. G., Onodera, T., Stein, M. M., Wang, T., Schachter, D. T., Hu, Z., and McMahon, P. L. Deep physical neural networks trained with backpropagation. *Nature*, 601(7894):549–555, 2022.
- Wycoff, J. F., Dillavou, S., Stern, M., Liu, A. J., and Durian, D. J. Desynchronous learning in a physics-driven learning network. *The Journal of Chemical Physics*, 156(14), 2022.
- Xiao, H., Rasul, K., and Vollgraf, R. Fashion-mnist: a novel image dataset for benchmarking machine learning algorithms. *arXiv preprint arXiv:1708.07747*, 2017.
- Xiao, T. P., Bennett, C. H., Feinberg, B., Agarwal, S., and Marinella, M. J. Analog architectures for neural network acceleration based on non-volatile memory. *Applied Physics Reviews*, 7(3), 2020.
- Xie, X. and Seung, H. S. Equivalence of backpropagation and contrastive hebbian learning in a layered network. *Neural computation*, 15(2):441–454, 2003.
- Yarotsky, D. Error bounds for approximations with deep relu networks. *Neural Networks*, 94:103–114, 2017.
- Yi, S.-i., Kendall, J. D., Williams, R. S., and Kumar, S. Activity-difference training of deep neural networks using memristor crossbars. *Nature Electronics*, 6(1):45–51, 2023.

A. Proofs

In this appendix, we prove the theoretical results. We proceed as follows:

- Theorem 2 is well known – we refer to Leshno et al. (1993) for a proof.
- First, we prove Lemma 3.
- Then, we prove Lemma 4 using Lemma 3.
- Then, we prove Theorem 5 using Lemma 3 and Lemma 4.
- Finally, we prove Theorem 1 using Theorem 2 and Theorem 5.

A.1. Proof of Lemma 3

For clarity, we repeat the lemma.

Lemma 3 (Equations of a DRN). *For every (ℓ, k) such that $1 \leq \ell \leq L - 1$ and $2 \leq k \leq N_\ell$, the equations for $v_k^{(\ell)}$ is*

$$p_k^{(\ell)} = \frac{\sum_{j=1}^{N_{\ell-1}} g_{jk}^{(\ell)} v_j^{(\ell-1)} + \sum_{j=1}^{N_{\ell+1}} g_{kj}^{(\ell+1)} v_j^{(\ell+1)}}{g_k^{(\ell)} + \sum_{j=1}^{N_{\ell-1}} g_{jk}^{(\ell)} + \sum_{j=1}^{N_{\ell+1}} g_{kj}^{(\ell+1)}} \quad (8)$$

$$v_k^{(\ell)} = \begin{cases} \max\left(0, p_k^{(\ell)}\right) & \text{if } k \text{ is even (excitatory unit),} \\ \min\left(0, p_k^{(\ell)}\right) & \text{if } k \text{ is odd (inhibitory unit).} \end{cases} \quad (9)$$

As for the equation of the output unit $v_k^{(L)}$,

$$v_k^{(L)} = \frac{\sum_{j=1}^{N_{L-1}} g_{jk}^{(L)} v_j^{(L-1)}}{g_k^{(L)} + \sum_{j=1}^{N_{L-1}} g_{jk}^{(L)}}, \quad 1 \leq k \leq q. \quad (10)$$

Proof of Lemma 3. Consider unit k in layer ℓ , with $0 < \ell \leq L$ and $1 \leq k \leq N_\ell$. First we consider the case $\ell < L$ of a hidden layer (we will consider the case $\ell = L$ of the output layer later). We denote $i_k^{(\ell)}$ the current flowing through the diode to the unit's node. The current flowing from ground to the unit's node through the resistor is $-g_k^{(\ell)} v_k^{(\ell)}$. We also denote $i_{jk}^{(\ell)}$ the current flowing from the j -th unit of layer $\ell - 1$ to the k -th unit of layer ℓ . Kirchhoff's current law (KCL) applied to the k -th unit of layer ℓ tells us that

$$i_k^{(\ell)} - g_k^{(\ell)} v_k^{(\ell)} + \sum_{j=1}^{N_{\ell-1}} i_{jk}^{(\ell)} - \sum_{j=1}^{N_{\ell+1}} i_{kj}^{(\ell+1)} = 0. \quad (27)$$

Furthermore, by Ohm's law we have $i_{jk}^{(\ell)} = g_{jk}^{(\ell)} (v_j^{(\ell-1)} - v_k^{(\ell)})$ and $i_{kj}^{(\ell+1)} = g_{kj}^{(\ell+1)} (v_k^{(\ell)} - v_j^{(\ell+1)})$. Therefore

$$i_k^{(\ell)} - g_k^{(\ell)} v_k^{(\ell)} + \sum_{j=1}^{N_{\ell-1}} g_{jk}^{(\ell)} (v_j^{(\ell-1)} - v_k^{(\ell)}) - \sum_{j=1}^{N_{\ell+1}} g_{kj}^{(\ell+1)} (v_k^{(\ell)} - v_j^{(\ell+1)}) = 0. \quad (28)$$

Solving (28) for $v_k^{(\ell)}$ we get

$$v_k^{(\ell)} = \frac{i_k^{(\ell)} + \sum_{j=1}^{N_{\ell-1}} g_{jk}^{(\ell)} v_j^{(\ell-1)} + \sum_{j=1}^{N_{\ell+1}} g_{kj}^{(\ell+1)} v_j^{(\ell+1)}}{g_k^{(\ell)} + \sum_{j=1}^{N_{\ell-1}} g_{jk}^{(\ell)} + \sum_{j=1}^{N_{\ell+1}} g_{kj}^{(\ell+1)}} \quad (29)$$

Now we use the characteristics of the diode between the unit's node and ground. First we consider the case of an excitatory unit ($v_k^{(\ell)} \geq 0$). We distinguish between two sub-cases: either $v_k^{(\ell)} > 0$ and $i_k^{(\ell)} = 0$ (the diode is in 'off-state'), or $v_k^{(\ell)} = 0$ and $i_k^{(\ell)} \geq 0$ (the diode is in 'on-state'). In the first sub-case (off-state) we have, using (29)

$$0 < v_k^{(\ell)} = \frac{\sum_{j=1}^{N_{\ell-1}} g_{jk}^{(\ell)} v_j^{(\ell-1)} + \sum_{j=1}^{N_{\ell+1}} g_{kj}^{(\ell+1)} v_j^{(\ell+1)}}{g_k^{(\ell)} + \sum_{j=1}^{N_{\ell-1}} g_{jk}^{(\ell)} + \sum_{j=1}^{N_{\ell+1}} g_{kj}^{(\ell+1)}}. \quad (30)$$

In the second sub-case (on-state) we have, using (29) again,

$$0 = v_k^{(\ell)} \geq \frac{\sum_{j=1}^{N_{\ell-1}} g_{jk}^{(\ell)} v_j^{(\ell-1)} + \sum_{j=1}^{N_{\ell+1}} g_{kj}^{(\ell+1)} v_j^{(\ell+1)}}{g_k^{(\ell)} + \sum_{j=1}^{N_{\ell-1}} g_{jk}^{(\ell)} + \sum_{j=1}^{N_{\ell+1}} g_{kj}^{(\ell+1)}}. \quad (31)$$

From (30) and (31) it follows that both sub-cases are captured by a single formula:

$$v_k^{(\ell)} = \max \left(0, \frac{\sum_{j=1}^{N_{\ell-1}} g_{jk}^{(\ell)} v_j^{(\ell-1)} + \sum_{j=1}^{N_{\ell+1}} g_{kj}^{(\ell+1)} v_j^{(\ell+1)}}{g_k^{(\ell)} + \sum_{j=1}^{N_{\ell-1}} g_{jk}^{(\ell)} + \sum_{j=1}^{N_{\ell+1}} g_{kj}^{(\ell+1)}} \right). \quad (32)$$

Similarly, an inhibitory unit satisfies

$$v_k^{(\ell)} = \min \left(0, \frac{\sum_{j=1}^{N_{\ell-1}} g_{jk}^{(\ell)} v_j^{(\ell-1)} + \sum_{j=1}^{N_{\ell+1}} g_{kj}^{(\ell+1)} v_j^{(\ell+1)}}{g_k^{(\ell)} + \sum_{j=1}^{N_{\ell-1}} g_{jk}^{(\ell)} + \sum_{j=1}^{N_{\ell+1}} g_{kj}^{(\ell+1)}} \right). \quad (33)$$

The case of output nodes ($\ell = L$) is identical, with $N_{L+1} = 0$ (meaning the layer of index $L + 1$ is empty) and $i_k^{(\ell)} = 0$ (no diode). Equation (29) rewrites in this case:

$$v_k^{(L)} = \frac{\sum_{j=1}^{N_{L-1}} g_{jk}^{(L)} v_j^{(L-1)}}{g_k^{(L)} + \sum_{j=1}^{N_{L-1}} g_{jk}^{(L)}} \quad (34)$$

□

A.2. Proof of Lemma 4

Lemma 4 (A maximum principle for DRNs). *For every ℓ such that $0 \leq \ell \leq L$, denote the maximum amplitude of electrical potential in layer ℓ as*

$$Z^{(\ell)} := \max_{1 \leq k \leq N_\ell} |v_k^{(\ell)}|. \quad (11)$$

Then we have

$$Z^{(\ell)} \leq Z^{(\ell-1)}, \quad 1 \leq \ell \leq L. \quad (12)$$

In particular, the electrical potentials of the units are bounded by the electrical potentials of input units:

$$|v_k^{(\ell)}| \leq \max_{1 \leq j \leq N_0} |v_j^{(0)}|, \quad 0 \leq \ell \leq L, \quad 1 \leq k \leq N_\ell. \quad (13)$$

Proof of Lemma 4. To prove (12), we proceed by induction on ℓ , starting from $\ell = L$, down to $\ell = 1$. We start with $\ell = L$. Using Lemma 3 we have for every k ,

$$|v_k^{(L)}| \leq \left| \frac{\sum_{j=1}^{N_{L-1}} g_{jk}^{(L)} v_j^{(L-1)}}{g_k^{(L)} + \sum_{j=1}^{N_{L-1}} g_{jk}^{(L)}} \right| \quad (35)$$

$$\leq \frac{\sum_{j=1}^{N_{L-1}} g_{jk}^{(L)} |v_j^{(L-1)}|}{g_k^{(L)} + \sum_{j=1}^{N_{L-1}} g_{jk}^{(L)}} \quad (36)$$

$$\leq \frac{\sum_{j=1}^{N_{L-1}} g_{jk}^{(L)} Z^{(L-1)}}{g_k^{(L)} + \sum_{j=1}^{N_{L-1}} g_{jk}^{(L)}} \quad (37)$$

$$\leq Z^{(L-1)}. \quad (38)$$

Since this holds for every k ($1 \leq k \leq N_L$), it follows that

$$Z^{(L)} \leq Z^{(L-1)}. \quad (39)$$

This completes the initialization step of the proof by induction. Suppose now that (12) holds for $\ell + 1$ where $2 \leq \ell + 1 \leq L$ and let's show the property for ℓ . Using again Lemma 3:

$$|v_k^{(\ell)}| \leq \left| \frac{\sum_{j=1}^{N_{\ell-1}} g_{jk}^{(\ell)} v_j^{(\ell-1)} + \sum_{j=1}^{N_{\ell+1}} g_{kj}^{(\ell+1)} v_j^{(\ell+1)}}{g_k^{(\ell)} + \sum_{j=1}^{N_{\ell-1}} g_{jk}^{(\ell)} + \sum_{j=1}^{N_{\ell+1}} g_{kj}^{(\ell+1)}} \right| \quad (40)$$

$$\leq \frac{\sum_{j=1}^{N_{\ell-1}} g_{jk}^{(\ell)} |v_j^{(\ell-1)}| + \sum_{j=1}^{N_{\ell+1}} g_{kj}^{(\ell+1)} |v_j^{(\ell+1)}|}{g_k^{(\ell)} + \sum_{j=1}^{N_{\ell-1}} g_{jk}^{(\ell)} + \sum_{j=1}^{N_{\ell+1}} g_{kj}^{(\ell+1)}} \quad (41)$$

$$\leq \frac{\sum_{j=1}^{N_{\ell-1}} g_{jk}^{(\ell)} Z^{(\ell-1)} + \sum_{j=1}^{N_{\ell+1}} g_{kj}^{(\ell+1)} Z^{(\ell+1)}}{g_k^{(\ell)} + \sum_{j=1}^{N_{\ell-1}} g_{jk}^{(\ell)} + \sum_{j=1}^{N_{\ell+1}} g_{kj}^{(\ell+1)}}. \quad (42)$$

Using the induction hypothesis, $Z^{(\ell+1)} \leq Z^{(\ell)}$, we get

$$|v_k^{(\ell)}| \leq \frac{\sum_{j=1}^{N_{\ell-1}} g_{jk}^{(\ell)} Z^{(\ell-1)} + \sum_{j=1}^{N_{\ell+1}} g_{kj}^{(\ell+1)} Z^{(\ell)}}{g_k^{(\ell)} + \sum_{j=1}^{N_{\ell-1}} g_{jk}^{(\ell)} + \sum_{j=1}^{N_{\ell+1}} g_{kj}^{(\ell+1)}}, \quad (43)$$

and since this holds for every $1 \leq k \leq N_\ell$, it follows that

$$Z^{(\ell)} \leq \frac{\sum_{j=1}^{N_{\ell-1}} g_{jk}^{(\ell)} Z^{(\ell-1)} + \sum_{j=1}^{N_{\ell+1}} g_{kj}^{(\ell+1)} Z^{(\ell)}}{g_k^{(\ell)} + \sum_{j=1}^{N_{\ell-1}} g_{jk}^{(\ell)} + \sum_{j=1}^{N_{\ell+1}} g_{kj}^{(\ell+1)}}. \quad (44)$$

Rearranging the terms, we get successively:

$$\left(g_k^{(\ell)} + \sum_{j=1}^{N_{\ell-1}} g_{jk}^{(\ell)} + \sum_{j=1}^{N_{\ell+1}} g_{kj}^{(\ell+1)} \right) Z^{(\ell)} \leq \sum_{j=1}^{N_{\ell-1}} g_{jk}^{(\ell)} Z^{(\ell-1)} + \sum_{j=1}^{N_{\ell+1}} g_{kj}^{(\ell+1)} Z^{(\ell)}, \quad (45)$$

$$\left(g_k^{(\ell)} + \sum_{j=1}^{N_{\ell-1}} g_{jk}^{(\ell)} \right) Z^{(\ell)} \leq \sum_{j=1}^{N_{\ell-1}} g_{jk}^{(\ell)} Z^{(\ell-1)}, \quad (46)$$

$$Z^{(\ell)} \leq Z^{(\ell-1)}. \quad (47)$$

This completes the induction step, and therefore completes the proof. \square

A.3. Proof of Theorem 5

Theorem 5 (Approximation of a ReLU NN with a DRN). *Suppose that, given an input signal $x = (x_1, x_2, \dots, x_{M_0})$, we set the input voltage sources to*

$$v_{2k}^{(0)} := A^{(0)} x_k, \quad v_{2k+1}^{(0)} := -A^{(0)} x_k, \quad 1 \leq k \leq M_0. \quad (23)$$

Denote $\|x\|_\infty := \max_{1 \leq k \leq M_0} |x_k|$. Then, in the limit $\gamma \rightarrow 0$, for every (ℓ, k) such that $1 \leq \ell \leq L - 1$ and $1 \leq k \leq M_\ell$, we have:

$$v_{2k}^{(\ell)} = A^{(\ell)} s_k^{(\ell)} + O(\gamma \|x\|_\infty), \quad (24)$$

$$v_{2k+1}^{(\ell)} = -A^{(\ell)} s_k^{(\ell)} + O(\gamma \|x\|_\infty), \quad (25)$$

$$v_k^{(L)} = s_k^{(L)} + O(\gamma \|x\|_\infty), \quad 1 \leq k \leq M_L. \quad (26)$$

Proof of Theorem 5. We prove the property (24) by induction on ℓ . It is true for $\ell = 0$ thanks to (23). Suppose that (24) is true for some $\ell - 1 \geq 0$ and let us prove it at the rank ℓ . Let k such that $1 \leq k \leq M_\ell$, and consider the excitatory unit $v_{2k}^{(\ell)}$ (the case of inhibitory unit $v_{2k+1}^{(\ell)}$, and the case of linear output unit $v_k^{(L)}$ if $\ell = L$, are similar). Recall from Lemma 3 that

$$v_{2k}^{(\ell)} = \max \left(0, \frac{\sum_{j=0}^{N_{\ell-1}} g_{j,2k}^{(\ell)} v_j^{(\ell-1)} + \sum_{j=1}^{N_{\ell+1}} g_{2k,j}^{(\ell+1)} v_j^{(\ell+1)}}{g_{2k}^{(\ell)} + \sum_{j=0}^{N_{\ell-1}} g_{j,2k}^{(\ell)} + \sum_{j=1}^{N_{\ell+1}} g_{2k,j}^{(\ell+1)}} \right). \quad (48)$$

First we calculate the denominator of expression (48). By distinguishing between the two cases $w_{jk}^{(\ell)} \geq 0$ or $w_{jk}^{(\ell)} \leq 0$, it is easy to see that we have in both cases:

$$g_{2j,2k}^{(\ell)} + g_{2j+1,2k}^{(\ell)} = \gamma^\ell |w_{jk}^{(\ell)}|. \quad (49)$$

Summing from $j = 0$ to $j = N_{\ell-1}$, we get the following formula for the denominator in (48),

$$\underbrace{g_{2k}^{(\ell)} + \sum_{j=0}^{N_{\ell-1}} g_{j,2k}^{(\ell)}}_{=\gamma^\ell a^{(\ell)}} + \underbrace{\sum_{j=1}^{N_{\ell+1}} g_{2k,j}^{(\ell+1)}}_{=O(\gamma^{\ell+1})} = \gamma^\ell a^{(\ell)} + O(\gamma^{\ell+1}). \quad (50)$$

Next, we calculate the numerator of (48). Similarly, whether $w_{jk}^{(\ell)} \geq 0$ or $w_{jk}^{(\ell)} \leq 0$, we have in both cases, using the inductive hypothesis:

$$g_{2j,2k}^{(\ell)} v_{2j}^{(\ell-1)} + g_{2j+1,2k}^{(\ell)} v_{2j+1}^{(\ell-1)} = \gamma^\ell A^{(\ell-1)} w_{jk}^{(\ell)} s_j^{(\ell-1)} + O(\gamma^{\ell+1}). \quad (51)$$

This identity also holds for $j = 0$ by defining $s_0^{(\ell-1)} := 1$ to include the case of the biases. Therefore

$$\sum_{j=0}^{N_{\ell-1}} g_{j,2k}^{(\ell)} v_j^{(\ell-1)} + \underbrace{\sum_{j=1}^{N_{\ell+1}} g_{2k,j}^{(\ell+1)} v_j^{(\ell+1)}}_{=O(\gamma^{\ell+1})} = \gamma^\ell A^{(\ell-1)} \left(\sum_{j=0}^{M_{\ell-1}} w_{jk}^{(\ell)} s_j^{(\ell-1)} \right) + O(\gamma^{\ell+1}). \quad (52)$$

Here we have used the maximum principle for $v_j^{(\ell+1)}$ (Lemma 4) to derive the bound $O(\gamma^{\ell+1})$. Finally, injecting (50) and (52) in (48) we obtain the following equation for $v_{2k}^{(\ell)}$:

$$v_{2k}^{(\ell)} = \max \left(0, \frac{A^{(\ell-1)}}{a^{(\ell)}} \left(\sum_{j=1}^{M_{\ell-1}} w_{jk}^{(\ell)} s_j^{(\ell-1)} + b_k^{(\ell)} \right) \right) + O(\gamma) = A^{(\ell)} s_k^{(\ell)} + O(\gamma). \quad (53)$$

The case of inhibitory unit $v_{2k+1}^{(\ell)}$ is similar: we obtain

$$v_{2k+1}^{(\ell)} = -A^{(\ell)} s_k^{(\ell)} + O(\gamma). \quad (54)$$

Hence, the property (24) is true at the rank ℓ . This completes the proof by induction. \square

A.4. Proof of Theorem 1

Theorem 1 (A universal approximation theorem for nonlinear resistive networks). *Given any continuous function $f : \mathbb{R}^p \rightarrow \mathbb{R}^q$, and given any compact subset $C \subset \mathbb{R}^p$ and any $\epsilon > 0$, there exists a nonlinear resistive network with p input voltage sources and q output branches such that, under the above assumptions of ideality, the function $F : \mathbb{R}^p \rightarrow \mathbb{R}^q$ that the nonlinear resistive network implements (i.e., the mapping between the inputs and outputs to the network) satisfies*

$$\|F(x) - f(x)\| \leq \epsilon, \quad \forall x \in C. \quad (1)$$

Proof of Theorem 1. Let $f : \mathbb{R}^p \rightarrow \mathbb{R}^q$ be a continuous function. Let C be a compact subset of \mathbb{R}^p , and let $\epsilon > 0$. By Theorem 2, there exists a ReLU neural network \mathcal{N} with p inputs and q outputs such that the function $G_{\mathcal{N}}$ that it implements satisfies

$$\|G_{\mathcal{N}}(x) - f(x)\| \leq \frac{\epsilon}{2}, \quad \forall x \in C. \quad (55)$$

Next, let $c := \max_{x \in C} \|x\|_\infty$, define $\gamma := \frac{\epsilon}{2c}$ and let \mathcal{R} the DRN approximator of \mathcal{N} with parameter γ (Section 3.3). By Theorem 5, the function $F_{\mathcal{R}}$ implemented by \mathcal{R} satisfies

$$\|F_{\mathcal{R}}(x) - G_{\mathcal{N}}(x)\| \leq \gamma \|x\|_\infty \leq \frac{\epsilon}{2}, \quad \forall x \in C. \quad (56)$$

Combining the two equations, we obtain

$$\|F_{\mathcal{R}}(x) - f(x)\| \leq \|F_{\mathcal{R}}(x) - G_{\mathcal{N}}(x)\| + \|G_{\mathcal{N}}(x) - f(x)\| \leq \epsilon, \quad \forall x \in C. \quad (57)$$

Hence the result. \square

B. Necessary conditions for universal function approximation

Our constructive proof of Theorem 1 demonstrates that the four circuit elements - voltage sources, resistors, diodes and VCVS - are *sufficient* for universal function approximation. In this appendix, we show that if either the diode or the VCVS is removed, the remaining three elements cannot achieve universal function approximation.

B.1. Necessity of diodes

We begin by demonstrating that an electrical circuit composed solely of ideal voltage sources, linear resistors, and ideal VCVS implements a linear input-output function.

Let M denote the number of edges in the circuit. We describe the state of the circuit using the set of branch voltages and branch currents, denoted as $v = (v_1, v_2, \dots, v_M)$ and $i = (i_1, i_2, \dots, i_M)$ respectively. The key point is that Kirchhoff's voltage law (KVL), Kirchhoff's current law (KCL) and the branch equations (current-voltage characteristics of the voltage sources, resistors, and VCVS) translate into linear equations involving v and i . Specifically, each constraint imposed by KVL is a linear constraint on the branch voltages, and each constraint imposed by KCL is a linear constraint on the branch currents. Ohm's law for resistors imposes a linear relationship between branch voltages and branch currents, and the current-voltage characteristic of the VCVS imposes a linear constraint on the branch voltages. Finally, voltage sources fix certain branch voltages to input values. Consequently, in such a circuit, the steady-state solution for branch voltages and branch currents is the solution of a system of linear equations in the input values. In particular, output voltages depend linearly on inputs.

Since nonlinearity is a prerequisite for universal approximation, these three elements alone - ideal voltage sources, linear resistors, and ideal VCVS - cannot serve as universal function approximators. This establishes the necessity of diodes in our construction.

B.2. Necessity of VCVS

Lemma 4 (the maximum principle for DRNs) establishes the necessity of VCVS in the DRN architecture: without amplification, output voltages are smaller than input voltages. Next, we generalize this result to any nonlinear resistive networks (Theorem 6 below).

We call a resistive device 'passive' if its current-voltage (i - v) characteristic satisfies $iv \geq 0$ at every operating point (i, v) . This definition encompasses the linear resistors and ideal diodes described in Section 2. A linear resistor obeys Ohm's law, $i = gv$, where $g \geq 0$ is the conductance, so $iv = gv^2 \geq 0$. In an ideal diode, either $i = 0$ or $v = 0$, ensuring that $iv = 0$.

Theorem 6. *In a circuit consisting only of ideal voltage sources and passive resistive devices, the voltage across any branch is bounded by the sum of sourced voltages.*

Theorem 6 implies that circuits with ideal voltage sources, linear resistors, and ideal diodes (without VCVS) cannot implement or approximate input-output functions for which outputs are larger in magnitude than the sum of inputs.

Proof of Theorem 6. We partition the network nodes into connected components: two nodes are in the same component if and only if a path of voltage source branches connects them. Let M_p^k represent the p -th node of the k -th connected component, and let N denote the number of such components. We construct a graph of N vertices, labeled A_1, A_2, \dots, A_N , each vertex being associated with a connected component of the electrical network. Between any two vertices A_j and A_k , a directed, weighted edge is drawn, with the edge's weight representing the total current flowing between the j -th and the k -th component, and the orientation corresponding to the direction of flow.

Let M_p^j and M_q^k be two nodes of the electrical network, and let v denote the voltage drop between them. From Lemma 7 (stated and proved at the end of this appendix), there is a directed path from A_j to A_k in the corresponding graph. Denote the length of this path as L . Up to re-indexing the connected components, we may assume $j = 0, k = L$, and that the path is $A_0 \rightarrow A_1 \rightarrow \dots \rightarrow A_L$. (By convention, $L = 0$ means that M_p^j and M_q^k belong to the same connected component). Back in the electrical network, this implies that, for each $\ell = 0, \dots, L - 1$, there exist network nodes M_s^ℓ and $M_t^{\ell+1}$ such that $M_s^\ell \rightarrow M_t^{\ell+1}$. Furthermore, by construction, for each ℓ , there exists a path of voltage source branches connecting M_t^ℓ to M_s^ℓ in the ℓ -th connected component. These resistive branches and voltage source branches form a path (in the electrical

network) from M_p^j to M_q^k . Applying Kirchhoff's voltage law (KVL) along this path, we have:

$$v + \sum_{b \in \mathcal{B}_R(M_p^j \rightarrow M_q^k)} v_b + \sum_{b \in \mathcal{B}_{VS}(M_p^j \rightarrow M_q^k)} v_b = 0, \quad (58)$$

where $\mathcal{B}_R(M_p^j \rightarrow M_q^k)$ and $\mathcal{B}_{VS}(M_p^j \rightarrow M_q^k)$ represent sets of resistive branches and voltage source (VS) branches, respectively, and v_b denotes the voltage across branch b . Let us examine the first term of the right-hand side of Eq. (58). By passivity of the resistors, $v_b i_b \geq 0$ for every resistor branch $b \in \mathcal{B}_R(M_p^j \rightarrow M_q^k)$, where i_b represents the current through b . Since the currents i_b are positive, the voltages v_b must also be positive, leading to:

$$v = - \sum_{b \in \mathcal{B}_R(M_p^j \rightarrow M_q^k)} v_b - \sum_{b \in \mathcal{B}_{VS}(M_p^j \rightarrow M_q^k)} v_b \leq - \sum_{b \in \mathcal{B}_{VS}(M_p^j \rightarrow M_q^k)} v_b \leq \sum_{b \in \mathcal{B}_{VS}} |v_b|, \quad (59)$$

where \mathcal{B}_{VS} denotes the set of all voltage source branches in the circuit. In the above reasoning, we can also invert the roles of M_p^j and M_q^k , and conclude that

$$-v \leq \sum_{b \in \mathcal{B}_{VS}} |v_b|. \quad (60)$$

Combining the two above inequalities, we get

$$|v| \leq \sum_{b \in \mathcal{B}_{VS}} |v_b|. \quad (61)$$

Hence the result. □

Finally, we state and prove Lemma 7, which we have used in the proof of Theorem 6.

Lemma 7. *Let G be a fully-connected edge-weighted directed graph with non-negative weights. Assume that flow conservation is satisfied at every vertex, meaning that, for each vertex, the sum of the incoming edge weights equals the sum of the outgoing edge weights. Then G is strongly connected, meaning that for any two vertices A and B of G , there exists $L \geq 0$ and a sequence of vertices A_1, A_2, \dots, A_L such that $A \rightarrow A_1 \rightarrow A_2 \rightarrow \dots \rightarrow A_L \rightarrow B$.*

Proof of Lemma 7. We proceed by induction on N , the number of vertices of the graph.

For the base case, let G be a graph with $N = 2$ vertices, denoted A and B . Flow conservation implies that there is no current flowing between A and B . Therefore, both $A \rightarrow B$ and $B \rightarrow A$ hold.

Next, suppose the property holds for $N \geq 2$ and consider a graph G with $N + 1$ vertices. Consider two vertices A and B of G . If $A \rightarrow B$, we are done. Otherwise, $B \rightarrow A$, and flow conservation at vertex B implies the existence of another vertex, say A_0 , such that $A_0 \rightarrow B$. We consider the reduced graph of N vertices, denoted \tilde{G} , in which A_0 and B are merged into a single vertex, denoted \tilde{B} , and weighted edges pointing towards and outwards of A_0 and B are merged with weights added. It is easy to see that the graph \tilde{G} also satisfies the property of flow conservation. Since \tilde{G} has N vertices, we can apply the induction hypothesis to \tilde{G} : there exists L and a directed path $A \rightarrow A_1 \rightarrow \dots \rightarrow A_L \rightarrow \tilde{B}$. Since $A_L \rightarrow \tilde{B}$ in \tilde{G} , this implies that either $A_L \rightarrow B$ or $A_L \rightarrow A_0$ in G . In the first case, $A \rightarrow A_1 \rightarrow \dots \rightarrow A_L \rightarrow B$ constitutes a directed path in G . In the second case, $A \rightarrow A_1 \rightarrow \dots \rightarrow A_L \rightarrow A_0 \rightarrow B$ constitutes a directed path. This completes the proof. □

C. Bidirectional amplifiers

One constraint of deep resistive networks (DRNs) is the decay in amplitude across the layers of the network, as the depth increases, and therefore the need to amplify the input voltages by a large gain $A^{(0)} \gg 1$ to compensate for this decay. Instead of amplifying input voltages by a large factor $A^{(0)}$, another solution proposed by Kendall et al. (2020) is to equip each ‘unit’ (or node) with a *bidirectional amplifier*.

A bidirectional amplifier is a three-terminal device, with bottom (B), left (L) and right (R) terminals. The bottom terminal is linked to ground. The current and voltage states (v_L, i_L) and (v_R, i_R) of the left and right terminals satisfy the relationship $v_R = a v_L$ and $i_R = a i_L$, for some positive constant a - the *gain* of the bidirectional amplifier. See Figure 4. Voltages are amplified in the forward direction by a factor $a > 1$, and currents are amplified in the backward direction by a factor $1/a$. In practice, a bidirectional amplifier can be formed by assembling a voltage-controlled voltage source (VCVS) and a current-controlled current source (CCCS).

We then equip each unit with a bidirectional amplifier, placed before the resistor and the diode (Figure 4). We define the unit’s state as the voltage after amplification. All the units of a given layer ℓ have the same gain $a^{(\ell)}$ as defined by (20). Lemma 3 can be restated as follows: for every (ℓ, k) such that $1 \leq \ell \leq L - 1$ and $1 \leq k \leq N_\ell$, the equation for $v_k^{(\ell)}$ is

$$v_k^{(\ell)} = \begin{cases} \max \left(0, \frac{\sum_{j=1}^{N_{\ell-1}} g_{jk}^{(\ell)} a^{(\ell)} v_j^{(\ell-1)} + \sum_{j=1}^{N_{\ell+1}} g_{kj}^{(\ell+1)} \frac{v_j^{(\ell+1)}}{a^{(\ell+1)}}}{g_k^{(\ell)} + \sum_{j=1}^{N_{\ell-1}} g_{jk}^{(\ell)} + \sum_{j=1}^{N_{\ell+1}} g_{kj}^{(\ell+1)}} \right) & \text{if } k \text{ is even (the unit is excitatory),} \\ \min \left(0, \frac{\sum_{j=1}^{N_{\ell-1}} g_{jk}^{(\ell)} a^{(\ell)} v_j^{(\ell-1)} + \sum_{j=1}^{N_{\ell+1}} g_{kj}^{(\ell+1)} \frac{v_j^{(\ell+1)}}{a^{(\ell+1)}}}{g_k^{(\ell)} + \sum_{j=1}^{N_{\ell-1}} g_{jk}^{(\ell)} + \sum_{j=1}^{N_{\ell+1}} g_{kj}^{(\ell+1)}} \right) & \text{if } k \text{ is odd (the unit is inhibitory).} \end{cases} \quad (62)$$

As for the equation of the output unit $v_k^{(L)}$,

$$v_k^{(L)} = \frac{\sum_{j=1}^{N_{L-1}} g_{jk}^{(L)} a^{(L)} v_j^{(L-1)}}{g_k^{(L)} + \sum_{j=1}^{N_{L-1}} g_{jk}^{(L)}}, \quad 1 \leq k \leq N_L. \quad (63)$$

In these expressions, $\frac{v_k^{(\ell)}}{a^{(\ell)}}$ and $\frac{v_j^{(\ell+1)}}{a^{(\ell+1)}}$ represent the units’ voltages before amplification.

Lemma 4 must also be adapted: with bidirectional amplifiers, the bounds depend not only on the input values (boundary conditions) but also on the layer-wise gains of the bidirectional amplifiers ($a^{(\ell)}$). Specifically, the equation for $Z^{(\ell)} := \max_{0 \leq j \leq N_\ell} |v_j^{(\ell)}|$ takes the following form:

$$Z^{(\ell)} \leq a^{(\ell)} Z^{(\ell-1)}, \quad 1 \leq \ell \leq L. \quad (64)$$

Multiplying by $A^{(\ell)} = a^{(\ell+1)} \times \dots \times a^{(L)}$ on both sides, we get

$$A^{(\ell)} Z^{(\ell)} \leq A^{(\ell-1)} Z^{(\ell-1)}, \quad 1 \leq \ell \leq L. \quad (65)$$

Iterating, we obtain:

$$A^{(\ell)} |v_k^{(\ell)}| \leq A^{(0)} \max_{1 \leq j \leq N_0} |v_j^{(0)}|, \quad 0 \leq \ell \leq L, \quad 1 \leq k \leq N_\ell. \quad (66)$$

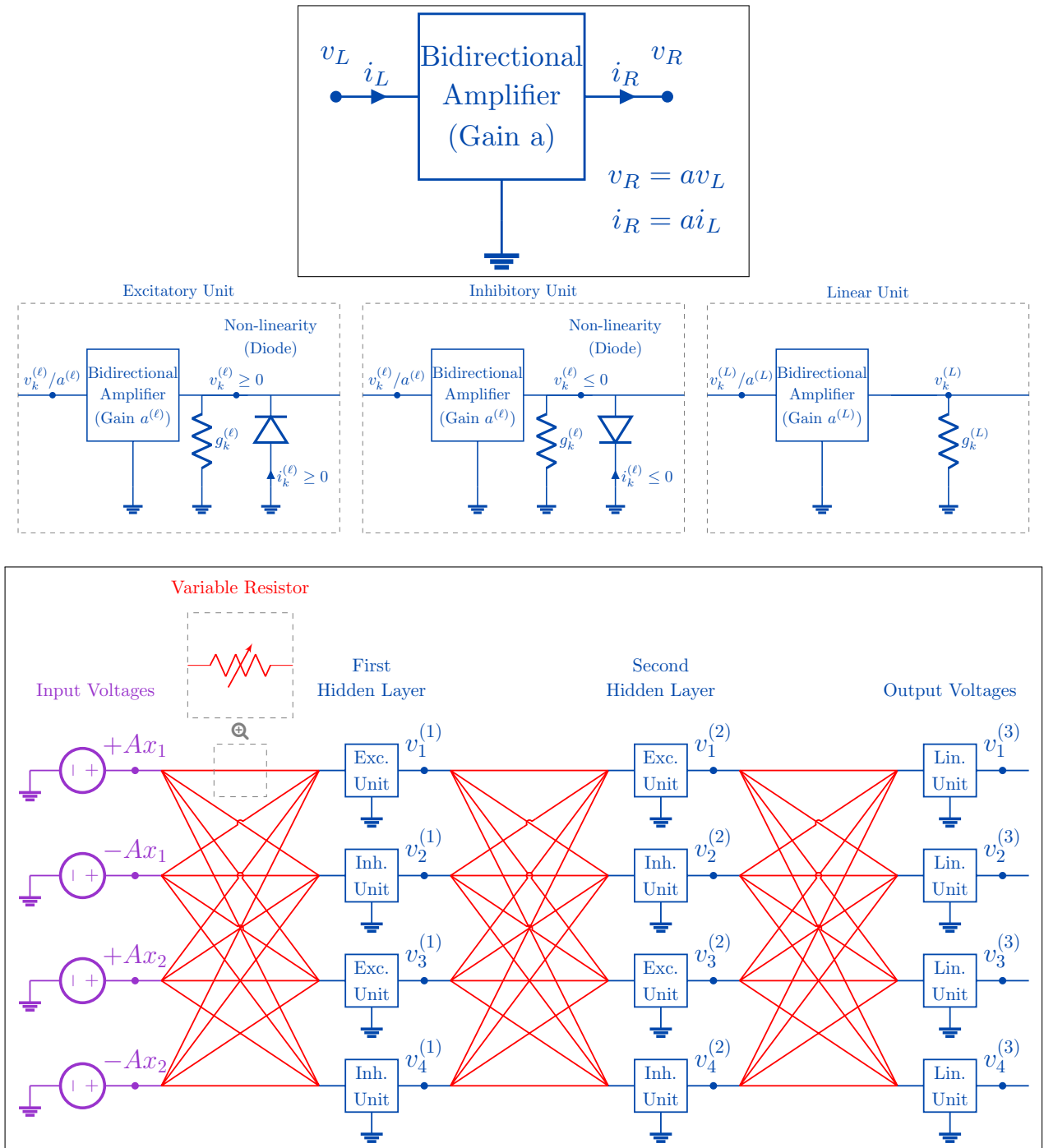


Figure 4. **Top left.** Bidirectional amplifier with gain a . **Top right.** One can form a bidirectional amplifier by combining a voltage-controlled voltage source (VCVS) and a current-controlled current source (CCCS). The right terminal voltage (v_R) is related to the left terminal voltage (v_L) by the relationship $v_R = av_L$, where a is a gain factor. The left terminal current (i_L) is related to the right terminal current (i_R) by the relationship $i_L = \frac{1}{a}i_R$. **Middle.** A unit is composed of a bidirectional amplifier (with amplification factor a), followed by a diode between the unit's node and ground. Depending on the orientation of the diode, units come in two flavours: excitatory units and inhibitory units. **Bottom.** A deep resistive network with bidirectional amplifiers.

D. Simulation details

In this appendix, we provide the details of our simulations (Section 4). We train DRNs with one, two and three hidden layers, and we compare their performances to their corresponding ReLU NNs with one, two and three hidden layers. Our code to reproduce the results is available at <https://github.com/rain-neuromorphics/energy-based-learning>

Datasets. We perform simulations on the MNIST, Kuzushiji-MNIST and Fashion-MNIST datasets.

The MNIST dataset (LeCun et al., 1998) consists of 60,000 training images and 10,000 test images. Each image is a 28x28 pixel grayscale representation of a handwritten digit ranging from 0 to 9. Each image is associated with a label indicating the digit it represents.

The Kuzushiji-MNIST dataset (Clanuwat et al., 2018) is a drop-in replacement for the MNIST dataset, also consisting of 60,000 training images and 10,000 test images, each a 28x28 pixel grayscale image. The images represent handwritten Kuzushiji (cursive Japanese) Hiragana characters. Like MNIST, each image in the Kuzushiji-MNIST dataset comes with an associated label, corresponding to Japanese characters.

The Fashion-MNIST dataset (Xiao et al., 2017) also features 60,000 training images and 10,000 test images. These images are also 28x28 pixels in grayscale, depicting various fashion items categorized into ten types such as shirts, trousers, and shoes.

Optimizer and scheduler. We optimize the MSE (mean squared error). We perform stochastic gradient descent (SGD) with momentum $\mu = 0.9$. No weight decay is used. We also use an ‘exponential learning rate scheduler’ with a decay rate of 0.99 for the learning rates at each epoch of training. We use mini batches of size 32 and we perform 100 epochs of training.

Computational resources. Our code for the simulations uses PyTorch 1.13.1 and TorchVision 0.14.1. (Paszke et al., 2017). The simulations were carried on three Nvidia A100 GPUs (one for each of the three sets of simulations corresponding to the three datasets). Each run took between 1 and 5 hours to complete, depending on the network type (DRN or ReLU NN) and network architecture (1H, 2H or 3H).

D.1. Simulation details of deep resistive networks (DRNs)

Table 3 contains the hyperparameters used to obtain the results presented in Table 1.

DRN architecture. We train deep resistive networks (DRNs) with one, two and three hidden layers, termed DRN-1H, DRN-2H and DRN-3H, respectively. Each DRN has 1568 input units ($2 \times 28 \times 28$), 10 output units and 1024 units per hidden layer. In our implementation for the simulations, we did not include resistors between the units’ nodes and ground (parallel to the diodes).

Input amplification factor. Input voltages are amplified by a (non-trainable) gain factor $A^{(0)}$. The value of $A^{(0)}$ is reported in Table 3 for each DRN architecture (DRN-1H, DRN-2H and DRN-3H).

Initialization of the conductances of the resistors. Given two consecutive layers of indices ℓ and $\ell + 1$, denoting N_ℓ the number of units in layer ℓ , we initialize the matrix $g^{(\ell+1)}$ of conductances between these two layers as

$$g_{jk}^{(\ell+1)} = \max\left(0, h_{jk}^{(\ell+1)}\right), \quad h_{jk}^{(\ell+1)} \sim \mathcal{U}(-c, +c), \quad c := \sqrt{\frac{1}{N_\ell}}. \quad (67)$$

Computing the steady state. We compute the steady state of the DRN with the following algorithm, introduced in Scellier (2024a). First we set the state of input units ($\ell = 0$) to their input values, and we initialize the state of the hidden layers and output layer to zero. Then, for $\ell = 1$ to $\ell = L - 1$, we perform the following operations. For every k such that $1 \leq k \leq N_\ell$, we update the state of unit $v_k^{(\ell)}$ as follows:

$$v_k^{(\ell)} \leftarrow \begin{cases} \max\left(0, p_k^{(\ell)}\right) & \text{if } k \text{ is even,} \\ \min\left(0, p_k^{(\ell)}\right) & \text{if } k \text{ is odd,} \end{cases} \quad \text{where} \quad p_k^{(\ell)} := \frac{\sum_{j=1}^{N_{\ell-1}} g_{jk}^{(\ell)} v_j^{(\ell-1)} + \sum_{j=1}^{N_{\ell+1}} g_{kj}^{(\ell+1)} v_j^{(\ell+1)}}{\sum_{j=1}^{N_{\ell-1}} g_{jk}^{(\ell)} + \sum_{j=1}^{N_{\ell+1}} g_{kj}^{(\ell+1)}}. \quad (68)$$

For the output layer ($\ell = L$), the update rule for the states of the output units $v_k^{(L)}$ is

$$v_k^{(L)} \leftarrow \frac{\sum_{j=1}^{N_{\ell-1}} g_{jk}^{(L)} v_j^{(L-1)}}{\sum_{j=1}^{N_{\ell-1}} g_{jk}^{(L)}}. \quad (69)$$

Importantly, we may update all the units of a given layer simultaneously, rather than sequentially, thus taking advantage of the parallelism of GPUs. Updating all the layers once, from inputs to output, constitutes one ‘iteration’. We perform T iterations of this process, until convergence to steady state. This algorithm is an instance of exact block coordinate descent.

Training procedure. We train our networks by stochastic gradient descent (SGD). At each training step, we proceed as follows. First we pick a mini-batch x of examples in the training set, and their corresponding labels y . Then we perform T iterations of the layer updates until convergence to the steady state. Once at steady state, we compute (or measure) the training error rate for the current mini-batch, to monitor training. Next, we perform another K iterations of the layer updates, and we compute the gradient of the cost function with respect to the weights (conductances) through the trajectory. This corresponds to a form of truncated backpropagation, where we perform $T + K$ steps in total, but we only backpropagate through the last K steps. Then, we update all the conductances simultaneously, proportionally to their gradient. Finally, we clip all the negative conductance values to zero, to ensure that all the conductances remain non-negative.

We also performed simulations using equilibrium propagation for extracting the conductance gradients, in place of (truncated) backpropagation. See Section D.3 below.

Table 3. Hyper-parameters used for initializing and training the deep resistive networks (DRNs) and reproducing the results of Table 1. lr means learning rate.

	DRN-1H	DRN-2H	DRN-3H
INPUT AMPLIFICATION FACTOR ($A^{(0)}$)	480	2000	4000
NUM. ITERATIONS AT INFERENCE (T)	4	5	6
NUM. ITERATIONS DURING TRAINING (K)	4	5	6
LR WEIGHT 1 & BIAS 1 (η_1)	0.006	0.002	0.005
LR WEIGHT 2 & BIAS 2 (η_2)	0.006	0.006	0.02
LR WEIGHT 3 & BIAS 3 (η_3)		0.005	0.08
LR WEIGHT 4 & BIAS 4 (η_4)			0.005
NUDGING PARAMETER (β), USED IN TABLE 4	0.5	1.0	2.0

D.2. Simulation details of ReLU neural networks (ReLU NNs)

As a baseline for our DRNs, we train ReLU NNs with one, two and three hidden layers, termed ReLU NN-1H, ReLU NN-2H and ReLU NN-3H, respectively.

ReLU NN architecture. Each of the three ReLU NN models has 784 input units (28×28), 10 output units, and 512 units per hidden layer.

Initialization of the weights. We use the ‘Kaiming uniform’ weight initialization scheme. Given two consecutive layers of indices ℓ and $\ell + 1$, denoting N_ℓ the number of units in layer ℓ , we initialize the matrix of conductances between these two layers as

$$w_{jk}^{(\ell+1)} \sim \mathcal{U}(-c, +c), \quad c := \sqrt{\frac{1}{N_\ell}}. \quad (70)$$

Computing the weight gradients. At each step of SGD, we calculate the weight gradients using backpropagation. We use $\eta = 0.005$ as a learning rate for all the weights and biases.

D.3. Extended simulation results

Table 1 presents the results we obtained using (truncated) backpropagation for training DRNs. Table 4 extends the results of Table 1 to include the results we obtained using equilibrium propagation (EP) for training. Table 4 also provides the error rates on the training set (training error rate), in addition to the test error rate.

In all cases, DRNs trained with BP achieve comparable test performance to their equivalent-size ReLU NNs. On the other hand, we observe that the training error rate in DRNs is often higher (sometimes significantly higher) than in ReLU NNs, hinting at an optimization issue for DRNs. We note however that our Theorem 5 only states the existence of a configuration of conductance values that approximates the behaviour of a ReLU NN at inference, but it does not provide any guarantee that this configuration of conductance values can easily be reached through gradient descent optimization. We also observe that DRNs trained with equilibrium propagation (EP) often achieve lower performance than with backpropagation (BP). Again, understanding these differences in performance is beyond the scope of our work. In this work, we provide a proof of existence, and we leave these open questions for future works to investigate.

Table 4. This Table provides a more extensive presentation of the results of Table 1. We compare the performance of DRNs trained with equilibrium propagation (DRN EP), DRNs trained with truncated backpropagation (DRN TBP), and their equivalent-size ReLU NNs trained with BP (ReLU NN BP). We train DRNs and ReLU NNs with one, two and three hidden layers on MNIST, Kuzushiji-MNIST and Fashion-MNIST. For each setting, we perform 5 runs and report the mean and std values of the training and test error rates.

DATASET	NETWORK MODEL (LEARNING ALGORITHM)	TEST ERROR (%)	TRAIN ERROR (%)
MNIST	DRN-1H (EP)	1.53 ± 0.05	0.07 ± 0.00
	DRN-1H (TBP)	1.51 ± 0.04	0.04 ± 0.00
	RELU NN-1H (BP)	1.67 ± 0.03	0.22 ± 0.01
	DRN-2H (EP)	1.60 ± 0.05	0.20 ± 0.01
	DRN-2H (TBP)	1.46 ± 0.05	0.20 ± 0.01
	RELU NN-2H (BP)	1.34 ± 0.01	0.03 ± 0.01
	DRN-3H (EP)	1.77 ± 0.08	0.36 ± 0.01
	DRN-3H (TBP)	1.47 ± 0.08	0.30 ± 0.01
	RELU NN-3H (BP)	1.48 ± 0.03	0.02 ± 0.00
KUZUSHIJI MNIST	DRN-1H (EP)	7.57 ± 0.11	0.08 ± 0.01
	DRN-1H (TBP)	7.67 ± 0.13	0.06 ± 0.00
	RELU NN-1H (BP)	8.83 ± 0.11	0.12 ± 0.01
	DRN-2H (EP)	8.40 ± 0.10	0.39 ± 0.03
	DRN-2H (TBP)	8.27 ± 0.02	0.42 ± 0.01
	RELU NN-2H (BP)	8.14 ± 0.13	0.05 ± 0.01
	DRN-3H (EP)	9.30 ± 0.17	0.63 ± 0.03
	DRN-3H (TBP)	8.39 ± 0.24	0.63 ± 0.01
	RELU NN-3H (BP)	7.99 ± 0.23	0.03 ± 0.01
FASHION MNIST	DRN-1H (EP)	10.38 ± 0.11	6.14 ± 0.15
	DRN-1H (TBP)	10.31 ± 0.05	5.91 ± 0.19
	RELU NN-1H (BP)	10.20 ± 0.11	5.13 ± 0.01
	DRN-2H (EP)	10.29 ± 0.14	6.20 ± 0.06
	DRN-2H (TBP)	9.88 ± 0.11	4.88 ± 0.05
	RELU NN-2H (BP)	9.42 ± 0.22	2.78 ± 0.03
	DRN-3H (EP)	11.23 ± 0.17	8.19 ± 0.05
	DRN-3H (TBP)	9.79 ± 0.25	4.58 ± 0.04
	RELU NN-3H (BP)	9.55 ± 0.14	1.82 ± 0.05

E. Equilibrium propagation

The deep resistive networks (DRNs) studied in this work were introduced within the Equilibrium Propagation (EP) training framework (Scellier & Bengio, 2017; Kendall et al., 2020). This appendix highlights the advantages that DRNs and EP offer over analog electrical implementations of neural networks using backpropagation (BP). We begin by discussing the challenges associated with analog implementations of BP.

E.1. Analog backpropagation

There has been a longstanding effort to develop analog versions of neural networks and backpropagation (BP). Most electrical implementations employ crossbar arrays of memristors to perform matrix-vector multiplications (MVMs) (Xiao et al., 2020), which constitute the core arithmetic operations of neural networks and BP. However, two additional operations are required: computing the nonlinear activation function, and computing its derivative. Based on whether these operations are executed in the analog or digital domain, analog implementations of BP can be broadly divided into two categories.

The first category aims to implement BP entirely in the analog domain, not just the MVMs. For instance, Hermans et al. (2015) utilized voltage followers to implement the ReLU activation function during the forward pass and analog switches to compute its derivative during the backward pass. However, this approach faces a significant challenge: analog devices cannot perfectly replicate the desired operations, leading to a mismatch between the activation function and its derivative. In practice, this mismatch will cause discrepancies between the calculated and actual weight gradients, leading to suboptimal optimization and reduced accuracy.

The second category employs mixed-signal (analog/digital) circuits, where MVMs are performed in the analog domain while nonlinear activation functions and their derivatives are computed digitally (Xiao et al., 2020). Such mixed-signal implementations of neural networks can mitigate the mismatch issue, however, the energy gains achieved by performing MVMs in the analog domain are offset by the power demands of analog-to-digital conversion (ADC) required before the activation function (Li et al., 2015).

Thus, it remains unclear whether BP is the most suitable training algorithm for analog computing platforms. This has led to the exploration of alternative approaches, such as EP, which may be better suited for these systems.

E.2. Equilibrium propagation

Equilibrium Propagation (EP), introduced in Scellier & Bengio (2017), has emerged as an alternative to backpropagation for training analog systems, including nonlinear resistive networks (Kendall et al., 2020). For a more general, physics-oriented overview of EP, see Scellier (2021). Here, we focus on EP’s application in DRNs, and explain how it addresses the mismatch problem found in analog BP.

EP is broadly applicable to energy-based systems that minimize an ‘energy’ (or Lyapunov) function. For deep resistive network with ideal components, the energy function corresponds to power dissipation:

$$E_{\text{DRN}}^{\text{ideal}}(v) = \sum_{\ell=1}^L \sum_{j=1}^{N_{\ell}} \sum_{k=1}^{N_{\ell+1}} g_{jk}^{(\ell)} \left(v_j^{(\ell)} - v_k^{(\ell+1)} \right)^2, \quad (71)$$

where $g_{jk}^{(\ell)}$ represents a memristor conductance, $v_j^{(\ell)}$ denotes a node electrical potential, and v is the vector of all node potentials. As shown by Scellier (2024a), these ideal DRNs reach a steady state v_* , given by:

$$v_* = \arg \min_{v \in \mathcal{S}_{\text{DRN}}^{\text{ideal}}} E_{\text{DRN}}^{\text{ideal}}(v), \quad (72)$$

where the feasible set $\mathcal{S}_{\text{DRN}}^{\text{ideal}}$ is defined by diode constraints:

$$\mathcal{S}_{\text{DRN}}^{\text{ideal}} = \{v \in \mathbb{R}^{\sum_{\ell=1}^L N_{\ell}} \mid v_k^{(\ell)} \geq 0 \text{ if } k \text{ is even, } v_k^{(\ell)} \leq 0 \text{ if } k \text{ is odd, } 1 \leq \ell \leq L-1, 1 \leq k \leq N_{\ell}\}. \quad (73)$$

In the present work, we have assumed ideal diodes to simplify the mathematical analysis of DRNs and derive our universal approximation theorem (specifically, this assumption has enabled us to derive Lemma 3 and subsequently an approximate equivalence with ReLU neural networks, Theorem 5). Similarly, Scellier (2024a) assumed ideal diodes to derive a fast algorithm to simulate DRNs on digital computers. Importantly however, EP does not rely on this assumption of ideality. In

fact, the i - v characteristics of nonlinear untrainable elements (diodes) do not need to be explicitly known. Indeed, nonlinear resistive networks with non-ideal elements possess an energy function called the ‘co-content’ (Millar, 1951) or ‘pseudo power’ (Kendall et al., 2020). For instance, the co-content for a DRN with linear resistors and non-ideal diodes is of the form:

$$E_{\text{DRN}}(v) = \sum_{\ell=1}^L \sum_{j=1}^{N_{\ell}} \sum_{k=1}^{N_{\ell+1}} g_{jk}^{(\ell)} \left(v_j^{(\ell)} - v_k^{(\ell+1)} \right)^2 + E_{\text{diodes}}(v), \quad (74)$$

where the term E_{diodes} depends solely on the i - v characteristics of the diodes. The steady state is then:

$$v_{\star} = \arg \min_v E_{\text{DRN}}(v). \quad (75)$$

The goal of learning is to minimize a cost function $C(v_{\star})$ with respect to the trainable weights (memristor conductances), given boundary input conditions from voltage sources. For example, using the mean squared error (MSE):

$$C(v) = \sum_k \left(v_k^{\text{out}} - y_k \right)^2, \quad (76)$$

where v_k^{out} is the k -th output node’s potential, and y_k is the k -th target output.

The core idea of EP is to interpret βC as power dissipation by resistors with conductance β linking output nodes to ‘target nodes’ (whose electrical potentials are set to target values). The resulting energy function (co-content) is:

$$F(v, \beta) = E_{\text{DRN}}(v) + \beta C(v), \quad (77)$$

where $\beta \geq 0$ is termed ‘nudging parameter’. Each training step of EP consists of:

1. Sourcing input voltages, setting $\beta = 0$ and allowing the system to reach the ‘free state’: $v_{\star}^0 = \arg \min_v F(0, v)$.
2. Increasing $\beta > 0$, and allowing the system to reach the ‘nudge state’: $v_{\star}^{\beta} = \arg \min_v F(\beta, v)$.

The gradient of the cost function with respect to the conductances can be estimated using the formula (Scellier & Bengio, 2017):

$$\frac{d}{dg} C(v_{\star}) = \frac{d}{d\beta} \bigg|_{\beta=0} \frac{\partial F}{\partial g} (v_{\star}^{\beta}, \beta) \approx \underbrace{\frac{1}{\beta} \left(\frac{\partial F}{\partial g} (v_{\star}^{\beta}, \beta) - \frac{\partial F}{\partial g} (v_{\star}^0, 0) \right)}_{=: \widehat{\nabla}_g(\beta)}. \quad (78)$$

Using the analytical form of the energy function, we obtain

$$\widehat{\nabla}_{g_{jk}^{(\ell)}}(\beta) = \frac{1}{\beta} \left(\frac{\partial F}{\partial g_{jk}^{(\ell)}} (v_{\star}^{\beta}, \beta) - \frac{\partial F}{\partial g_{jk}^{(\ell)}} (v_{\star}^0, 0) \right) = \frac{1}{\beta} \left[\left((v_j^{(\ell)})^{\beta} - (v_k^{(\ell+1)})^{\beta} \right)^2 - \left((v_j^{(\ell)})^0 - (v_k^{(\ell+1)})^0 \right)^2 \right]. \quad (79)$$

Finally, we update the weights (memristor conductances) using these gradient estimates, to perform (or approximate) one step of gradient descent on the cost function:

$$\Delta g = -\eta \widehat{\nabla}_g(\beta). \quad (80)$$

The learning rule for each weight (memristor) is local, and notably, it is agnostic to the i - v characteristics of the diodes. Whether the network components are ideal or non-ideal, the EP algorithm and its learning rules remain unchanged. This feature makes EP robust to variability of analog devices, particularly untrainable nonlinear elements (diodes), which is a key advantage of DRNs and EP over analog implementations of neural networks and BP. Intuitively, the robustness of EP arises because the same network is used for both phases of training (free and nudge), so that non-idealities affect both states similarly and thus cancel out in the gradient calculation. EP thus solves the mismatch problem encountered in BP between the nonlinear activation function and its derivative.

In addition to the resistive networks considered in this work, EP has been applied to various energy-based systems, such as continuous Hopfield networks (Scellier & Bengio, 2017), Ising machines (Laydevant et al., 2024) and coupled phase oscillators (Wang et al., 2024). A variant of EP called Coupled learning has been developed and used in other systems as

well, such as flow and elastic networks (Stern et al., 2021; Altman et al., 2024). Recent works have extended EP to quantum systems too (Massar & Mognetti, 2024; Wanjura & Marquardt, 2024b; Scellier, 2024b).

While EP's learning rule does not require knowledge of the characteristics of untrainable elements, it does require knowledge of the partial derivatives of the energy function with respect to trainable weights ($\frac{\partial E}{\partial g}$). However, a more advanced version of EP called 'Agnostic Equilibrium Propagation' (AEP) has been introduced, which does not require knowledge of these partial derivatives either, and allows to perform the weight updates using physical dynamics (Scellier et al., 2022).